Prepared for

NATIONAL AERONAUTICS AND SPACE ADMINISTRATION
Headquarters
Washington, D. C. 20546

by

Dr. F. F. Marmo, Project Director and
Principal Investigator

April 1966

EXPERIMENTAL AND THEORETICAL STUDIES
IN PLANETARY AERONOMY

Quarterly Progress Report

Covering the Period 1 January 1966
through 31 March 1966

Prepared under Contract No. NASW-1283

TABLE OF CONTENTS

Section	Title	Page
I	INTRODUCTION	1
II	TECHNICAL SUMMARIES OF WORK PERFORMED UNDER THE PRESENT CONTRACT	3
	A. Photochemistry of Planetary Atmospheres	3
	1. The Role of $O(^1D)$ in Reactions with O_3	3
	2. The Reaction of $O(^1D)$ with Nitrogen	8
	B. Laboratory Investigations in the VUV and the EUV Spectral Regions	11
	1. The Mass Analysis of Photoionization Products	11
	2. Electron Energy Spectrum Due to EUV and VUV Photoionization	11
	3. Atomic Hydrogen Photoionization Cross Sections	16
	4. Absorption and Photoionization Cross Sections	20
	C. Planetary Aeronomy	23
	1. Experimental Investigations	23
	a. Chemiluminescence from Selected Planetary Gases for $\lambda\lambda < 3000$Å	23
	b. Fluorescence from Molecular Oxygen Excited by Lyman-Alpha, 1215.7Å	27
	2. Theoretical Studies	27
	a. Model Atmospheres of Mars	27
	b. A Satellite Experiment on the Detection of Noctilucent Clouds in the VUV Region	38
III	OTHER PERTINENT INFORMATION	50
	REFERENCES	52

I. INTRODUCTION

This is the Fourth Quarterly Progress Report which describes the technical progress from 1 January 1966 through 31 March 1966 under NASA Contract No. NASW-1283. Scientific investigations accomplished during the current reporting period resulted in the generation of the following papers submitted and/or accepted for publication in accredited scientific journals, books and/or GCA Technical Reports or presented at scientific meetings.

Technical Papers Submitted and/or Accepted for Publication

	Publication
a. Submitted	
Ionization Potential of Molecular Xenon and Krypton (J.A.R. Samson and R. B. Cairns)	J. Opt. Soc. Am.
b. Accepted	
CO_2 Actinometer for Argon Source (P. Warneck)	J. Opt. Soc. Am. 56, 408 (1966)
Ionization Potential of O_2 (J.A.R. Samson and R. B. Cairns)	J. Opt. Soc. Am.
Gas Analysis by Photoionization Mass Spectrometry (W. Poschenrieder and P. Warneck)	J. Applied Phys.
Total Absorption Cross Sections of CO and CO_2 in the Region 550-200Å (R. B. Cairns and J.A.R. Samson)	J. Opt. Soc. Am.

Technical Papers Presented at Scientific or Professional Meetings

A Study of the Kinetic Energies of Electrons Produced by Photoionization (J.A.R. Samson and R. B. Cairns) — Presented by J.A.R. Samson at the Fiftieth Anniversary Meeting of the Optical Society of America held in Washington, D.C., on March 15-18, 1966.

In Section II, technical summaries are given on the work performed under the present contract. During the current reporting period, significant progress has been achieved in the following areas:

A. Photochemistry of planetary atmospheres

B. Laboratory investigations in the VUV and the EUV spectral regions

C. Planetary aeronomy

D. Other pertinent information.

II. TECHNICAL SUMMARIES OF WORK PERFORMED UNDER THE PRESENT CONTRACT

A. PHOTOCHEMISTRY OF PLANETARY ATMOSPHERES

1. The Role of $O(^1D)$ in Reactions with O_3

In this work, the photolysis of oxygen at 1470Å is utilized to produce $O(^1D)$ simultaneously with $O(^3D)$, and the production of ozone is investigated as a function of pressure and temperature. A number of data obtained were reported in the last quarterly report but no analysis had been accomplished at that date. The required kinetic analysis of these data has now been performed and the results are given below.

The kinetic mechanism on which the quantitative analysis is based can be written

$$O_2 + h\nu \xrightarrow{1470\text{Å}} O + O^* \qquad (1)$$

$$O + 2\,O_2 \rightarrow O_3 + O_2 \quad \text{fast} \qquad (2)$$

$$O^* + 2\,O_2 \rightarrow O_3 + O_2 \quad k_3 \qquad (3)$$

$$O^* + O_2 \rightarrow O_2 + O \quad k_4 \qquad (4)$$

$$O^* + O_3 \rightarrow 2\,O_2 \quad k_5 \qquad (5)$$

where O^* signifies excited oxygen atoms in the ^1D metastable state. Treating the reaction space next to the light source window as a stirred reaction leads to the equations

$$\frac{v\,\Delta\,(O_3)}{R} = \frac{I}{R} + (k_3 + k_4)(O_2)(O^*) - k_5(O_3)(O^*) \qquad (6)$$

$$\frac{v \, \Delta \, (O^*)}{R} = \frac{I}{R} - O^* \; [(k_3 + k_4)(O_2) + k_5(O_3)] \tag{7}$$

Here, the concentrations refer to the outgoing (steady-state) concentrations, v is the flow rate, R the reactor volume and I the integrated light intensity. If the oxygen atoms formed in the primary process (1) are nearly all consumed in the reactor, the term $v \, \Delta \, (O^*)/R$ becomes negligible. The resulting ozone concentration is obtained from the quadratic equation

$$(O_3)^2 + \frac{[k_3(O_2) + k_4]}{k_5} \, (O_2)(O_3) - \frac{2I}{k_5 v} \, [k_3(O_2) + k_4] \; (O_2) = 0 \; . \tag{8}$$

Upon introducing the ozone quantum yield $q = (O_3) \, v/I$, we obtain the expression

$$\frac{q^2}{2-q} \, \frac{I}{v} = \frac{k_3(O_2) + k_4}{k_5} \, (O_2) \tag{9}$$

which relates the experimental parameters q, I, v and (O_2) with the ratios of rate constants k_3/k_5 and k_4/k_5. Accordingly, if the function on the left-hand side of this equation is plotted versus pressure, a straight line should be obtained at low pressures where $k_3(O_2) \ll k_4$. Such a plot is shown in Figure 1 for the data obtained at room temperature. Indeed, a linear relationship is observed for pressures below 250 mm Hg. The increasing nonlinearity at higher pressures indicates the influence of Reaction (3). Rate constant ratios k_4/k_5 are then obtained from the slope of the linear portion, and Table 1 provides a list of the averaged values obtained for three different temperatures.

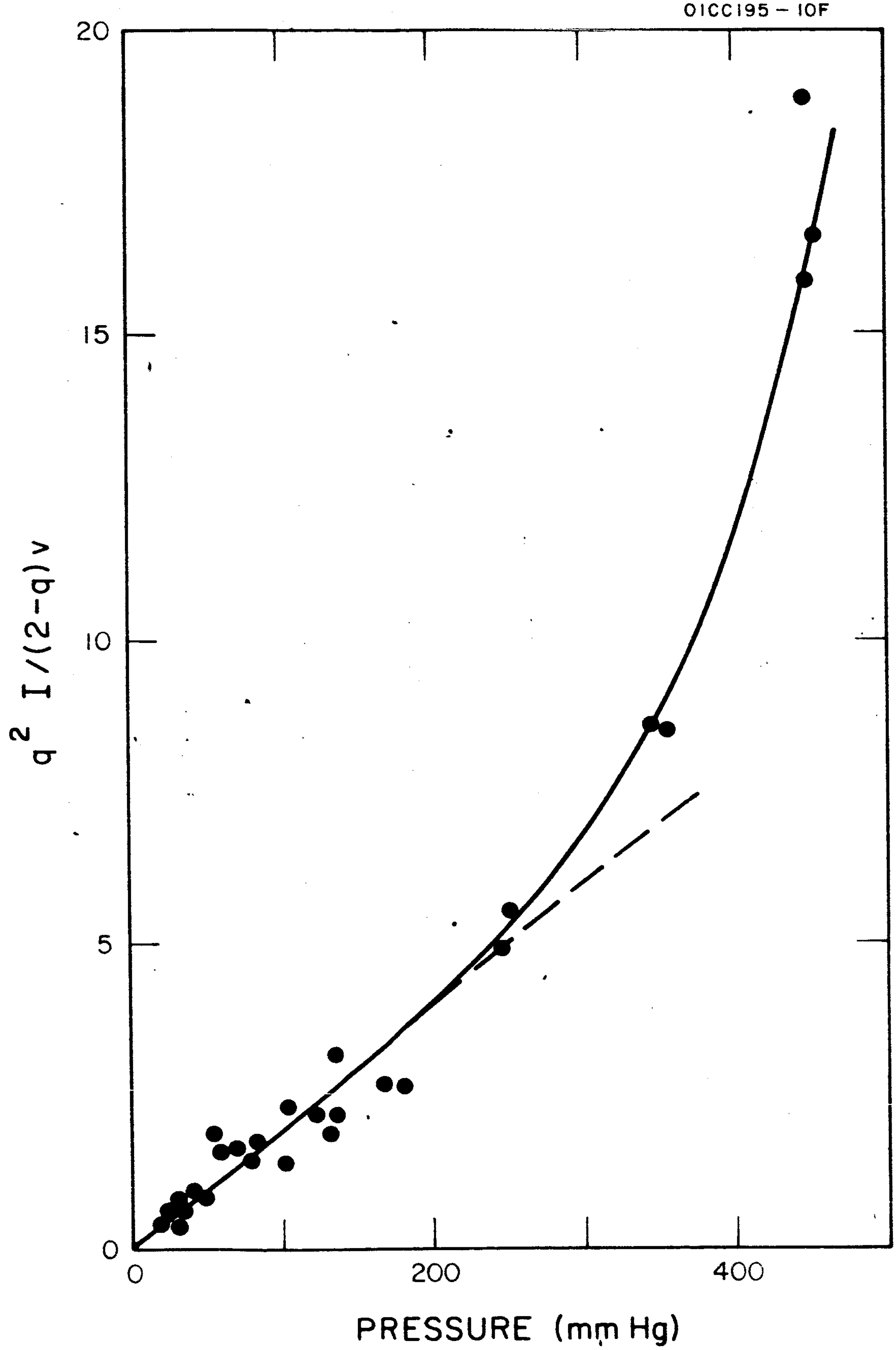

Figure 1. Pressure dependence of ozone quantum yields expressed in the form $q^2 I/(2-q)v$.

TABLE 1

$T(^{o}C)$	$T(^{o}K)$	k_4/k_5
0	273	$(0.91 \pm 0.23) \times 10^{-3}$
24	297	$(0.61 \pm 0.12) \times 10^{-3}$
50	223	$(0.47 \pm 0.15) \times 10^{-3}$

To obtain the activation energy of Reaction (5), it is assumed that the deactivation of $O(^1D)$ by Reaction (4) proceeds with negligible temperature dependence. Figure 2 shows a semi-logarithmic plot of k_5/k_4 versus the reciprocal temperature. A straight line is obtained indicating a relationship $k_5 = k_5^* \exp(-E/RT)$. From the slope of the line, the activation energy E is found to be E = 2,400 ± 1,400 cal.

Returning to Equation (9), one can now insert the deduced average values for k_4/k_5 for each temperature and determine an average value for k_3/k_5 (here assumed to be temperature independent) from the data at pressures above 250 mm Hg. The value here found is $k_3/k_5 = (2.1 \pm 1.1)\ 10^{-23}$ cc/molecules.

A brief discussion is in order concerning these results. At a first glance, it appears that nothing can be said about the absolute magnitude of the individual rate constants, since only ratios can be determined within the framework of photolytic work. However, upper and lower limits can be given in relation to other data available from the literature. Considering k_4/k_5, it is seen that from the values given in Table 1, that k_5

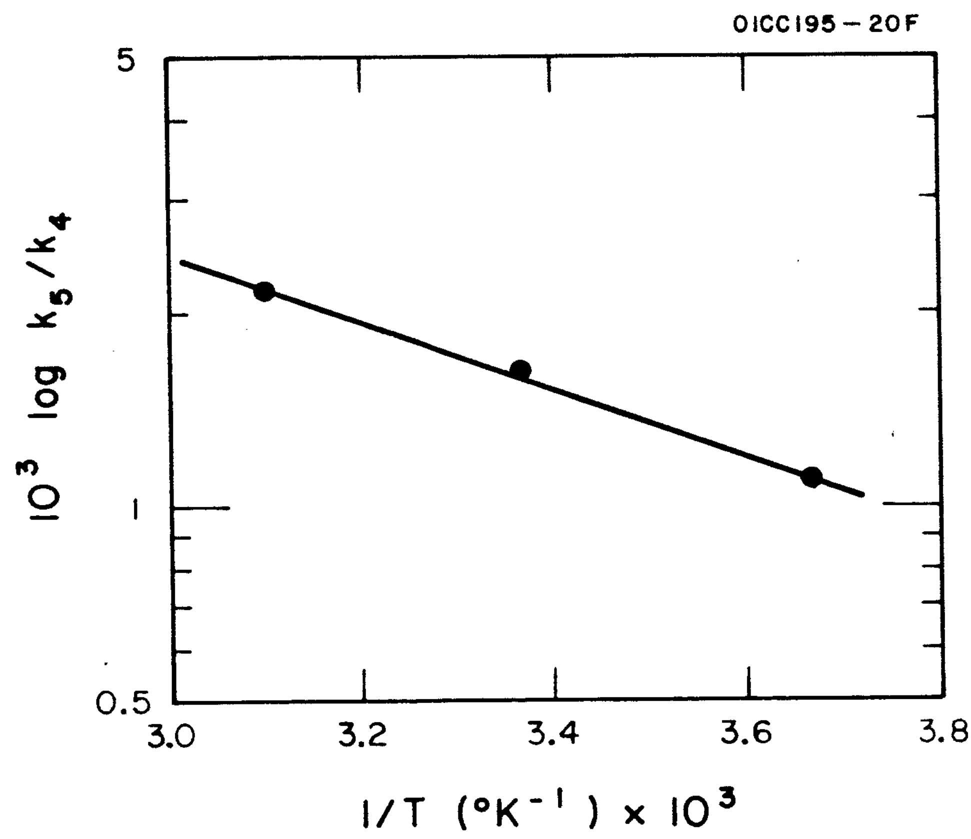

Figure 2. Temperature dependence of k_5/k_4.

is more than a thousand times greater than k_4. The upper limit of k_5 is given by the collision frequency of $k_5 \leq 2.5 \times 10^{-10}$ cc/molecules sec. This puts an upper limit on the deactivation rate constant of $k_4 \leq 10^{-13}$ cc/molecules sec. On the other hand, Hunten and McElroy[1] have made an analysis of the gas discharge data by Kvifte and Vegard[2] concerning the emission by $O(^1D)$ with the result that $k_4 \approx 10^{-15}$ cc/molecules sec. Accordingly, from our data $k_5 \approx 2 \times 10^{-12}$ cc/molecules sec. However, the present results also provide the activation energy associated with Reaction (5). Setting $k_5 = k_5^* \exp(-2{,}400/RT)$ with $k_5^* = 2.5 \times 10^{-10}$, the value obtained at room temperature is $k_5 = 4 \times 10^{-12}$ cc/molecules sec, in reasonable agreement with the value given above. Hence, k_5 is much faster than the corresponding rate constant for the reaction of ^3P ground oxygen atoms. By contrast, k_3 is much smaller. Taking $k_5 = 4 \times 10^{-12}$ gives $k_3 = 8 \times 10^{-35}$ cc/molecules sec, which is by about an order of magnitude smaller than the rate constant value for ozone formation by ^3P oxygen atoms. Partial support for the problem of $O(^1D)$ deactivation by O_2 was received under Contract No. NASw-1341.

2. The Reaction of $O(^1D)$ with Nitrogen

While the results concerning the reaction of $O(^1D)$ atoms with ozone are reasonably complete, there remains to investigate the reaction with nitrogen. Data concerning the deactivation of $O(^1D)$ by nitrogen have been obtained in conjunction with the above work, although an analysis of these data must still be performed. Here, however, we are concerned with the reaction with nitrogen leading to the formation of N_2O. As deMore and Raper[3] have shown, this reaction is much slower than the deactivation reaction between the same reactants. Consequently, only a negligible production of N_2O can be expected.

It was previously proposed to study the reaction $O(^1D) + N_2 \rightarrow N_2O$ by photolysis of a mixture of CO_2 and N_2, and to detect N_2O by means of mass spectrometry. The choice of this system was predicated upon our previous findings[4,5] that CO_2 photolysis produces $O(^1D)$ oxygen atoms and that their reaction with nitrogen is fast in comparison to that with carbon dioxide. From more recent data reported by Cvetanovic,[8] it appears that the reaction with CO_2 is rapid, whereas our present results show that the reaction with N_2 is slow. This has two consequences: (a) the CO_2 photolysis system is unsuitable for the contemplated study, and (b) the use of mass spectrometric analysis of N_2O is not sufficiently sensitive. These new factors suggest that an isotype scheme employing mass spectrometric measurements must be abandoned in favor of an alternative scheme. In the search for other appropriate study methods, it has become apparent that the photolysis of ozone in the presence of large amounts of nitrogen provides a suitable system, and that mass spectrometry as the analytical tool should be replaced by gas chromatography. A brief analysis of the expected mechanism follows. As deMore and Raper[3,6] have shown, the photolysis of ozone at 2537Å yields $O(^1D)$ oxygen atoms in the primary step. Norrish and Wayne[7] have recently found that in the presence of excess nitrogen, the ozone quantum yield declines towards two, indicating that most of the $O(^1D)$ oxygen atoms responsible for additional O_3 destruction are deactivated. The mechanism, accordingly, can be written

$$O_3 + h\nu \rightarrow O + O^{+}$$

$$O^* + N_2 \xrightarrow{k_2} N_2 + O$$

$$\xrightarrow{k_2} N_2O$$

$$O + O_3 \xrightarrow{k_3} 2\ O_2$$

with O^* signifying oxygen atoms in the excited (^1D) state. It follows from a steady-state treatment that

$$\frac{\Delta\ N_2O}{\Delta t} = k_2(N_2)(O^*) = \frac{k_2}{k_1+k_2}\ I_a$$

$$\frac{\Delta\ O_3}{\Delta t} = I_a + k_2(O)(O_3) = I_a\ \frac{(2\ k_1 + k_2)}{k_1 + k_2} \approx 2$$

$$\frac{\Delta\ N_2O}{\Delta\ O_3} = \frac{k_2}{2\ k_1 + k_2} \approx \frac{k_2}{2\ k_1}$$

so that the ratio of rate constants for Reactions (1) and (2) can be obtained from a determination of the ozone consumption and the N_2O production, provided both are measurable quantities. The former measurement is easily accomplished by absorption photometry. For the latter, a gas chromatograph should be used. From a statement of Norrish and Wayne,[7] the detection of N_2O appears to be just within the realm of possibility.

B. LABORATORY INVESTIGATIONS IN THE VUV (1000-2000Å) AND THE EUV (BELOW 1000Å) SPECTRAL REGIONS

1. The Mass Analysis of Photoionization Products

This portion of the program has been completed. The results have been accepted for publication in the Journal of Applied Physics and is to appear in the June 1966 issue.

2. Electron Energy Spectrum Due to EUV and VUV Photoionization

The electron energy analyzer reported in the last Quarterly has been tested and found to produce good results with a limiting energy resolution of approximately 3 percent. That is, the energies of a group of electrons whose energies are in the vicinity of 10 eV can be identified if their energy separation is more than 0.3 eV. This resolution is sufficient to identify most electronic states of a molecule and some of the vibrational states.

The most important advance in this study is that with the present techniques, we have been able to use monochromatic radiation with only a 5Å bandpass to produce electrons within the analyzer. Thus, a considerable amount of valuable information should be forthcoming. The importance of this technique is that for the first time one can now give the probability that a photon of a given energy will be absorbed in a particular molecular state. These data are directly applicable to current views on the aeronomy of the upper atmosphere. As an example, we have determined the individual absorption processes in our test gas xenon. Figure 3 shows the raw data as obtained directly from the analyzer. It reveals two steps in the electron

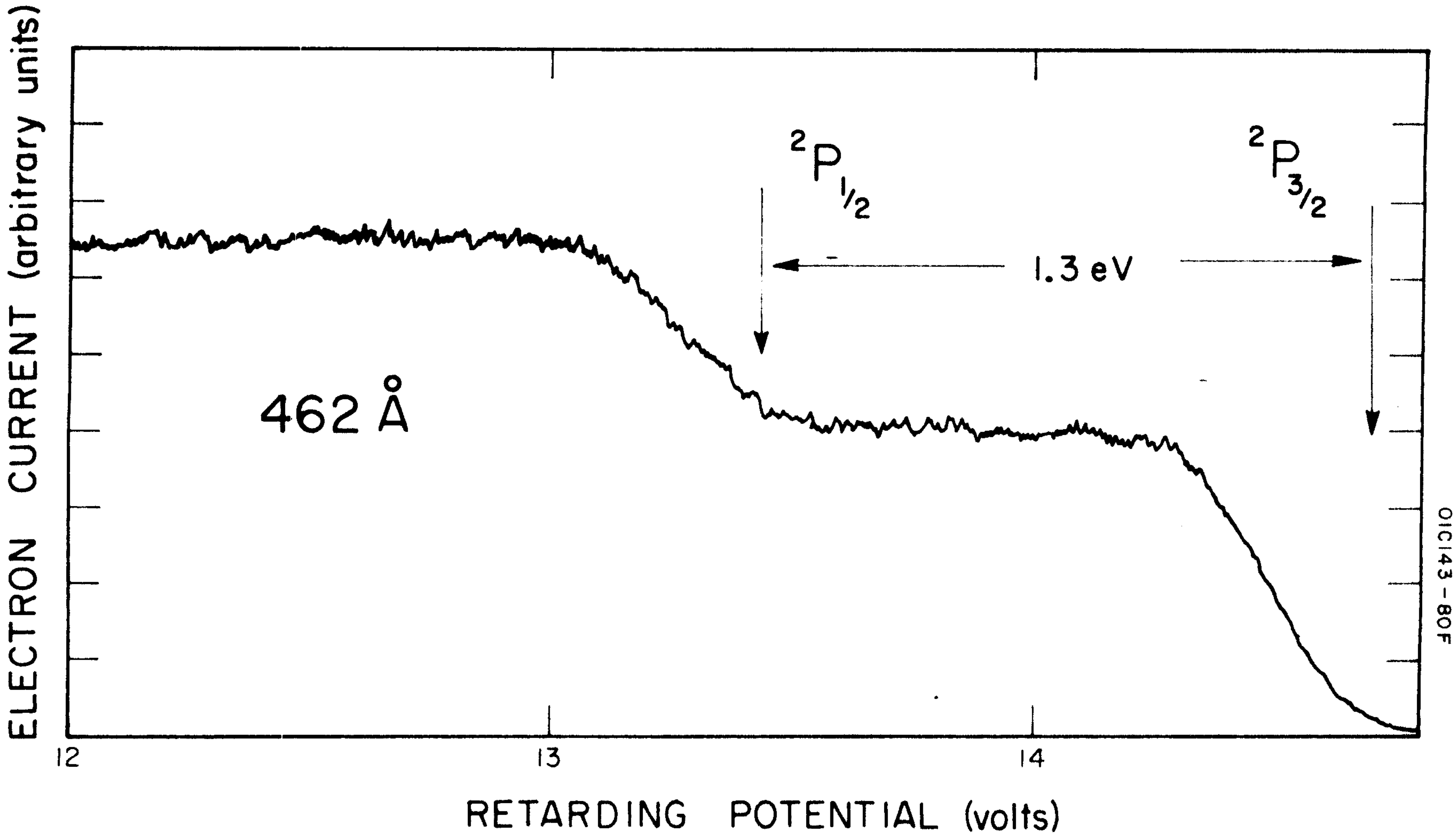

Figure 3. Electron current as a function of retarding potential for electrons produced by the photoionization of xenon at a wavelength of 462Å.

current as the retarding potential is increased; the ratio of the heights of these steps is equal to the ratio of the absorption cross sections for the two absorption processes which leave the ion in its $^2P_{3/2}$ ground state and its $^2P_{1/2}$ excited state. The results as a function of wavelength are shown in Figure 4 down to 400Å. The symbols $\sigma_{1/2}$, etc., refer to the specific absorption cross sections for the $^2P_{1/2}$, $^2P_{3/2}$, and the total absorption cross sections.

Referring back to Figure 3, the sloping portions of the step should ideally be vertical. The slope indicates the energy resolution of the analyzer. In the case of molecules, a more gentle slope (i.e., apparently poorer resolution) would indicate other absorption processes which were unresolved. Figure 5 shows such a condition for molecular nitrogen. Radiation of 570Å wavelength is absorbed by nitrogen into its ground X $^2\Sigma_g^+$ state and into the excited states A $^2\Pi_u$ and B $^2\Sigma_u^+$. Again the magnitude of the steps is indicative of the most probable transition. In this case, the most probable transition is into the A $^2\Pi_u$ state. This state contains many vibrational levels which are not resolved at present as is evident from the slowly rising step into this transition (Figure 5).

A major problem still to be solved is the effect of the earth's magnetic field on very slow electrons. During the next Quarter, we plan to build a Helmholtz coil to counteract the effect of the earth's field. We also hope to improve the energy resolution of the analyzer and its sensitivity.

The material discussed has been presented as a paper entitled "A Study of the Kinetic Energies of Electrons Produced by Photoionization"

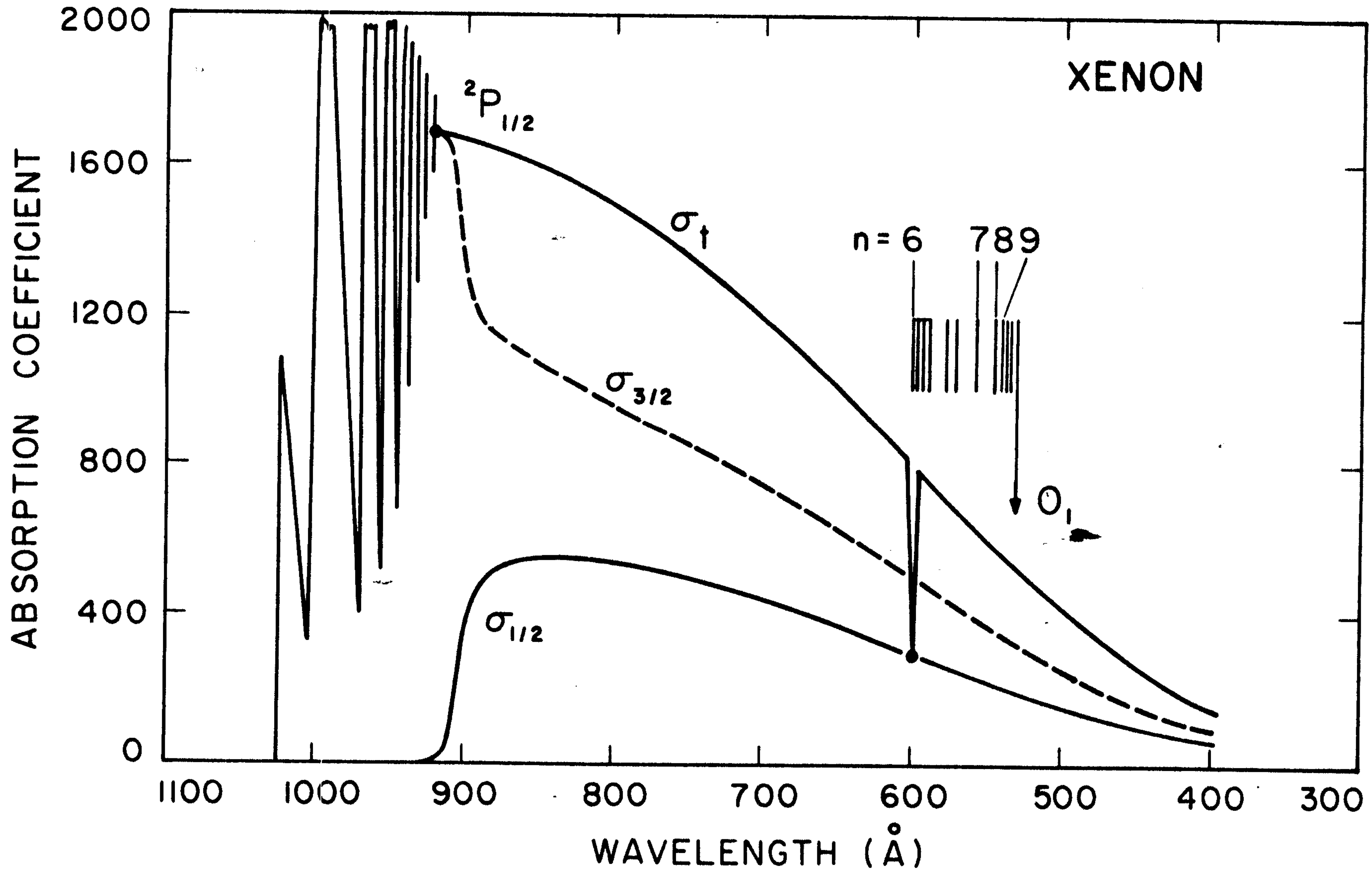

Figure 4. The specific absorption coefficients for xenon. σ_t denotes the total absorption coefficient.

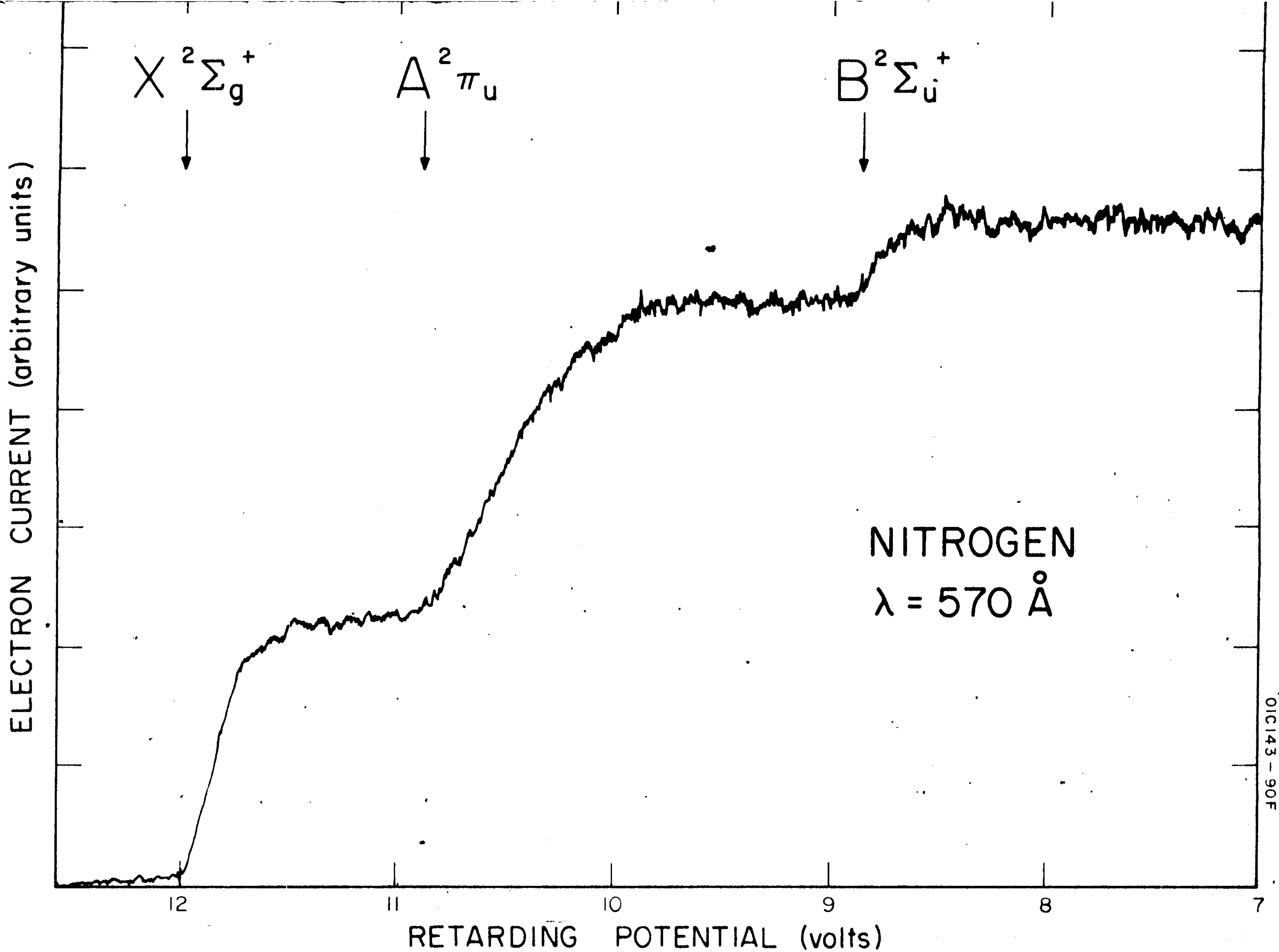

Figure 5. Electron current as a function of the retarding potential for electrons produced by the photoionization of nitrogen at a wavelength of 570Å. The transitions to several electronic states are clearly indicated.

by J. A. R. Samson and R. B. Cairns at the Fiftieth Anniversary Meeting of the Optical Society of America on March 17, 1966, in Washington, D. C.

3. Atomic Hydrogen Photoionization Cross Sections

As previously reported, experiments have been undertaken to determine the most efficient method for producing large numbers of hydrogen atoms. Radio frequency discharges of several frequencies and microwave discharges have been studied. The various techniques produce similar degrees of dissociation and as a result, microwave discharges are being used because of their compactness and simplicity of operation. The Wrede-Harteck method of measuring the number density of atoms has been used. Although this method is capable of measuring the atom density in the vicinity of the gauge, it does not provide a value for the total number of hydrogen atoms per cm^2-column in a flowing system where pressure gradients exist. Thus, the original experiment was envisaged with a Wrede-Harteck gauge at both ends of the absorbing gas column. This would allow a mean atom density to be determined and hence the total number of absorbing atoms. However, a new and novel technique has been developed which obviates this complicated experimental procedure. This new method permits the atom cross section to be determined without any knowledge of the number of absorbing atoms. It is thought that this constitutes the first occasion upon which a cross section has been measured without such information. The method is simple, providing only two absorbing species are present; namely, ground state H_2 and H. Present evidence in the literature and from our laboratory suggests that this is the case.

Consider first a measurement of the relative absorption cross section of H at two frequencies ν_1 and ν_2.

At ν_1

$$\frac{\ln I_o}{I_1} = L\, \sigma_{(H_2\nu_1)}\, N_{(H_2)}$$

where only H_2 is present, L is the length of the absorbing column, $\sigma_{(H_2\nu_1)}$ is the molecular absorption cross section, $N_{(H_2)}$ is the number density of H_2, and I_o/I_1 is the ratio of the light intensities incident and transmitted through the gas. With the discharge on, and both H_2 and H absorbing,

$$\ln \frac{I_o}{I_2} = L\left[\sigma_{(H_2\nu_1)}\, N'_{(H_2)} + \sigma_{(H\ \nu_1)}\, N'_{(H)}\right]$$

where I_2 is now the transmitted light intensity, $\sigma_{(H\ \nu_1)}$ is the atom cross section, and $N'_{(H_2)}$ and $N'_{(H)}$ are the number densities of H_2 and H, respectively.

We have:

$$N_{(H_2)} = N'_{(H_2)} + \frac{1}{2} N'_{(H)}$$

$\therefore$ Eliminating $N'_{(H_2)}$,

$$\frac{1}{L} \ln \frac{I_o}{I_2} = \left[\sigma_{(H_2\nu_1)} \left(N_{(H_2)} - \frac{1}{2} N'_{(H)}\right) + \sigma_{(H\ \nu_1)}\, N'_{(H)}\right]$$

or

$$\frac{1}{L} \ln \frac{I_o}{I_2} = \frac{1}{L} \ln \frac{I_o}{I_1} - \frac{1}{2}\, \sigma_{(H_2\nu_1)}\, N'_{(H)} + \sigma_{(H\ \nu_1)}\, N'_{(H)} ;$$

i.e.,

$$\frac{1}{L} \ln \frac{I_1}{I_2} = N'_{(H)} \left[\sigma_{(H\ \nu_1)} - \frac{1}{2} \sigma_{(H_2\nu_1)} \right] \tag{10}$$

At frequency ν_2

$$N'_{(H)} \left[\sigma_{(H\ \nu_2)} - \frac{1}{2} \sigma_{(H_2\nu_2)} \right] = \frac{1}{L} \ln \frac{i_1}{i_2} \tag{11}$$

Dividing Equation (10) by Equation (11)

$$\frac{\sigma_{(H\ \nu_1)} - \frac{1}{2} \sigma_{(H_2\nu_1)}}{\sigma_{(H\ \nu_2)} - \frac{1}{2} \sigma_{(H_2\nu_2)}} = \frac{\ln I_1/I_2}{\ln i_1/i_2} \ . \tag{12}$$

Since I_1, I_2, i_1, i_2, $\sigma_{(H_2\nu_1)}$, and $\sigma_{(H_2\nu_2)}$ are measured quantities, the relative values of $\sigma_{(H)}$ at frequencies ν_1 and ν_2 are known. It should be noted that the $N'_{(H)}$ does not appear in Equation (12).

Once the relative cross sections are known, it remains to normalize the data by knowing the absolute cross section at one point.

Reference to Equation (10) shows that if $\sigma_{(H\ \nu_1)} = \frac{1}{2} \sigma_{(H_2\nu_1)}$, then $\ln \frac{I_1}{I_2} = 0$; i.e., $I_1 = I_2$. Experimentally, this means that the intensity of the transmitted light is unaltered when the discharge is switched on. When this occurs, therefore, the cross section of the atom is known to equal one-half of the molecular cross section which can be measured; thus, the curve σ_H versus λ can be made absolute without knowing $N'_{(H)}$.

Preliminary data for the relative cross sections are available at wavelengths between 900 and 800Å. Below 800Å, molecular hydrogen absorbs more strongly creating experimental difficulties which have yet to be properly surmounted. A graph is given of the theoretical cross section and the present tentative data which have, in this case, been normalized to fit the theoretical curve at 900Å (see Figure 6).

Experiments are continuing to extend and improve this work, and a parallel experiment - in which any long-lived ions produced in discharged H_2 could be detected - is under way. This experiment is to verify the supposition that only H_2 and H are the absorbing species in the discharged gas.

4. Absorption and Photoionization Cross Sections

The ionization potentials of Xe_2 and Kr_2 have been determined, the latter being measured for the first time.

Interpretation of the new data indicates that the production of ions in xenon and krypton by resonance line absorption can be ascribed to:

$$Xe + h\nu \rightarrow Xe^*$$

followed by

$$Xe^* + Xe \rightarrow Xe_2^* \rightarrow Xe_2^+ + e + KE .$$

which has been verified in the case of the alkali metals.

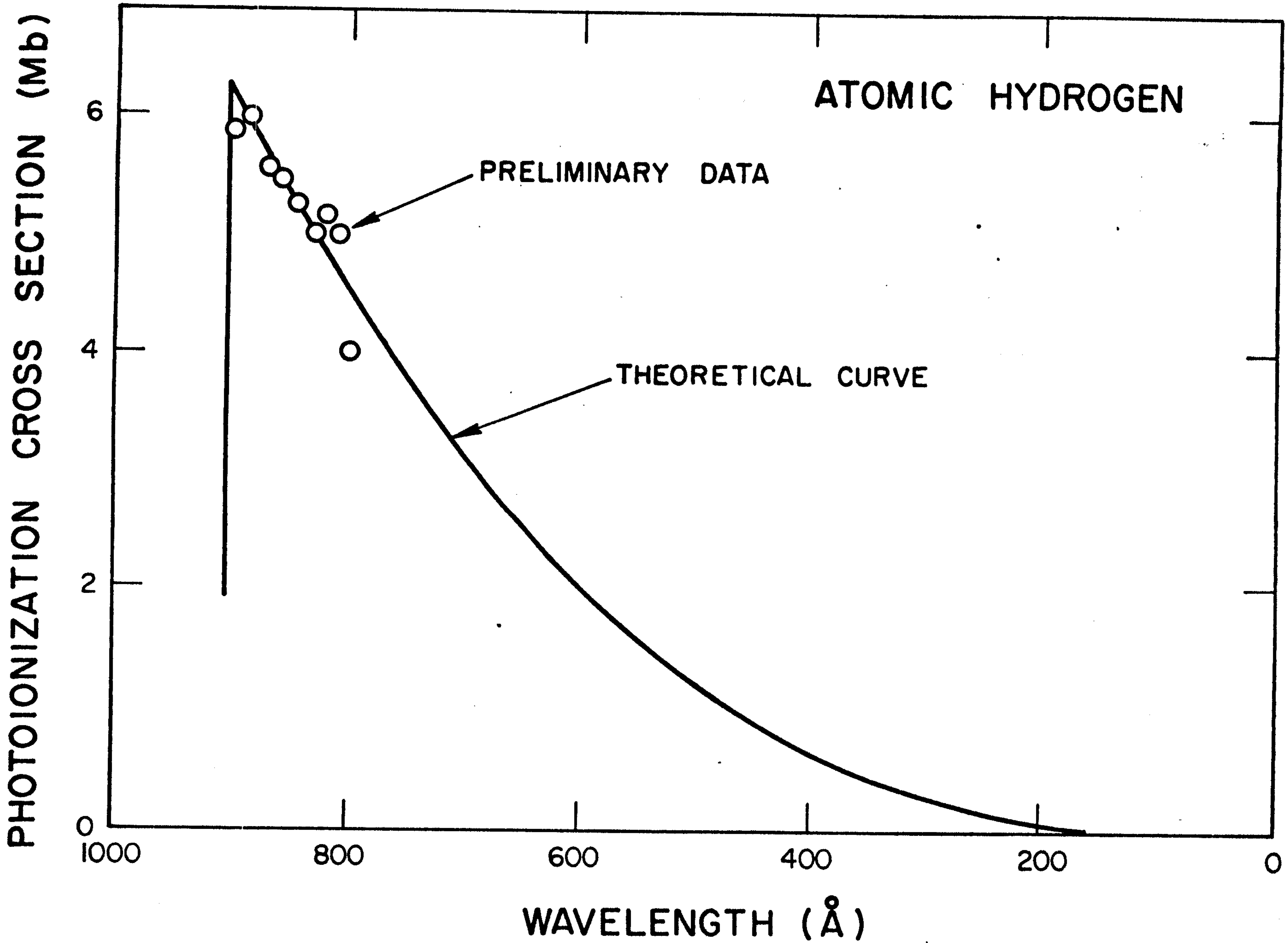

Figure 6. The photoionization cross section of atomic hydrogen.

— theoretical values;

○ preliminary experimental data.

The many-lined spectrum of molecular hydrogen was used as a photon source, while dispersion of the radiation was achieved by a 1/2 m Seya monochromator with a wavelength resolution of 0.7Å. A windowless ion chamber with a pathlength of 28 cm was employed to investigate the ionization resulting from resonance line absorption by both xenon and krypton, although a lithium fluoride window was used at higher xenon pressures to study the direct excitation and ionization of Xe_2. Research grade gas was used at pressures ranging from 1 to 300 torr. Ion currents of the order of 10^{-12} A were obtained at wavelengths corresponding to the following resonance line absorptions: $mp^6\ {}^1S$ - nd $[3/2]^o$, (n + 1) d $[3/2]^o$, (n + 2) s $[1/2]^o$, and (n + 3) s $[3/2]^o$, where for Xe, n = 5, 6, ...etc. and m = 5, for Kr, n = 4, 5, ...etc. and m = 4. At higher pressures, ionization was observed to occur at wavelengths lying between resonance lines and is attributed to either direct ionization of the rare gas molecule or excitation of the molecule followed by an autoionizing transition into the continuum state of the molecular ion.

Ions first appeared at 963.37Å in krypton corresponding to the 4p - 5d resonance transition so that the ionization potential of Kr_2 must be $\leq$ 12.87 eV (963.37Å). Melton and Hamill obtained an appearance potential of 13.2 ± .02 eV while Hornbeck and Molnar quote a value of $13.23\,^{+\,0.3}_{-\,0.7}$ eV.

In the case of xenon, the first resonance transition which produced ionization was the 5p - 6d transition at 1110.71Å. However, the appearance potential of ions at high pressure (10 to 100 torr) was at 1112.7 ± 2Å. Thus, it is concluded that the ionization potential of Xe_2 is 11.14 ± 0.02 eV (1112.7 ± 2Å).

The dissociation energy of the ground state of Xe_2 is, therefore, 0.99 ± 0.02 eV; for Kr_2, the dissociation energy is $\geq$ 1.06 eV.

C. PLANETARY AERONOMY

1. Experimental Investigations

a. Chemiluminescence from Selected Planetary Gases for $\lambda\lambda < 3000\text{Å}$

The vacuum ultraviolet chemiluminescence survey has been completed and is reported as follows.

Recent shock-tube experiments have shown that there is vacuum-ultraviolet emission from the reaction of oxygen with acetylene.[9] Hand[10] identified the emission from an oxyacetylene burner in the region 1810 to 2220Å as part of the fourth positive carbon monoxide band system ($A^1\Pi$). This identification led him to suggest that the emission observed in the shock-tube experiments was also due to the fourth positive carbon monoxide bands, although the principal emission in that case was in the region 1500 to 1700Å which could not be studied by Hand because of the molecular oxygen cutoff at 1800Å. Most recently in this laboratory, the fourth positive carbon monoxide bands in the vacuum ultraviolet were identified during the "cold" reaction of atomic oxygen with acetylene.[11] Present interest has grown into the possibility of vacuum ultraviolet emission from the reaction of other hydrocarbons as well as planetary gases with atomic species. With this in mind, a survey-type investigation was carried out utilizing various hydrocarbons and possible planetary gases with atomic oxygen, atomic nitrogen and atomic hydrogen.

A conventional fast flow system was used throughout the entire survey. Atomic oxygen was produced by passing a 99:1 mixture of argon-oxygen through a microwave discharge. The atomic hydrogen was produced in much the same way, by passing a 99:1 mixture of argon-hydrogen through the microwave discharge. Molecular nitrogen alone through the discharge sufficed for the production of an ample amount of atomic nitrogen.

The atomic species and studied reactants were mixed in a reaction cell which was maintained at a pressure of 800 microns of mercury. Adjacent to the mixing point, a nitric-oxide-filled GM counter was installed with its lithium fluoride window inside the reaction cell. Previous studies undertaken in this laboratory have utilized a GM counter or a photon counter outside the reaction cell. This necessitated a second lithium fluoride window as well as a flushing system to minimize molecular oxygen absorption between the two windows. With the present arrangement, losses of radiation due to the above absorption as well as the transmission through the second window are omitted and a lower detection limit is obtained. Since this investigation is primarily a survey, no slit arrangement was incorporated and the solid angle viewed by the GM counter was very large.

Listed in Table 2 are the observations of the reactions of atomic oxygen and various compounds. In all of the observed reactions, the the fourth positive carbon monoxide bands are the emitters. However, since some radiation is obtained with ammonia gas, it is conjectured that a small quantity of hydrocarbon is present with the gas. It is of some significance to note that the relative intensity of the radiation is dependent upon the chemical bond of the reactant species; i.e., triple bond is the most intense, double bond the next, and single bond the least.

TABLE 2

Relative Intensities of Chemiluminescent Vacuum Ultraviolet Radiation

Reactant	Atomic Oxygen	Atomic Nitrogen	Atomic Hydrogen
Acetylene	1000	0	0
Allene	100	0	0
Ammonia	0.1	0	0
Carbon Dioxide	0	0	0
Carbon Monoxide	0	0	0
Carbonyl Chloride	0	0	0
Carbonyl Sulfide	0	0	0
Ethane	1	0	0
Ethylene	10	0	0
Hydrogen Sulfide	0	0	0
Methane	0	0	0
Methyl Acetylene	100	0	0
Nitric Oxide	0	0	0
Nitrogen Dioxide	0	0	0
Sulfur Dioxide	0	0	0

Employing molecular nitrogen alone through the microwave discharge for the production of atomic nitrogen resulted in a very high observed counting rate even before the admission of any of the reactant gases. It has been ascertained that this radiation is due to the Lyman-Birge-Hopfield band system of nitrogen. This system has been readily observed in both absorption and emission and has been identified in the N_2 afterglow by Tanaka.[12] Since the contribution of this radiation is so large (greater than a thousand times original background), a true evaluation of the existence of any resulting reaction with the reactants is not anticipated. However, a survey was attempted to ascertain whether any reactant would appreciably increase the counting rate. None of the reactants did.

A second attempt was made with a mixture of nitrogen and argon passing through the microwave discharge. The background counting rate was lowered (as was the atomic nitrogen concentration), but again no increase in radiation was observed with any of the reactants.

No radiation was observed when mixing various reactants with atomic hydrogen. The flows of both the reactant and atomic hydrogen were varied as well as the ambient pressure without any change in the counting rate.

Although vacuum-ultraviolet radiation was observed only in the reactions between some hydrocarbons and atomic oxygen, one cannot definitely rule out a reaction between the other compounds and atomic oxygen as well as other atomic species. Since the entire wavelength span of the nitric oxide GM counter is only about 300Å (1050 to 1340Å), radiation still may exist beyond this 1340Å limit. A photomultiplier tube which encompasses a larger wavelength range (1050 to 2000Å) would be applied as a suitable detector for a more extensive study. In addition, absolute intensity values would establish upper limits to specific reaction rates to apply to vacuum ultraviolet airglow in the earth and other planetary atmospheres.

b. Fluorescence from Molecular Oxygen Excited by Lyman-Alpha, 1215.7Å

Several alternative schemes have been proposed for the origin of oxygen airglow in the earth's upper atmosphere. In addition, some of these have been closely allied to the Hertzberg emissions due to molecular O_2. In an effort to reduce the various possibilities, the following rather straightforward experiment was performed.

The McPherson VUV monochromator was employed with a hydrogen light source to yield about 10^9 photons sec^{-1} (at 1215.7Å) at the exit slit where an O_2 gas-filled cell with lithium fluoride windows was placed. A photomultiplier probe was employed to detect any fluorescence emitted from the excited O_2. The pressure range investigated varied from a few mm up to one atmosphere. The results were negative in that no observable fluorescence was detected although the system was capable of detecting as little as 10^5 photons sec^{-1}. Although the experiment is not conclusive, it can be used to establish a limiting value on the fluorescence of O_2 in the upper atmosphere excited by the solar Lyman-alpha line.

2. <u>Theoretical Studies</u>

a. Model Atmosphere of Mars

Mariner IV occultation measurements have provided some new data concerning the surface pressure, temperature and refractivity of the atmosphere of Mars. These measurements show that the atmosphere essentially consists of carbon dioxide with a number density of $1.9 \pm 1 \times 10^{17}$ molecules per cc and a temperature of $180 \pm 20^{\circ}K$ at a reference level close to the surface. No significant change in scale height was observed in the lower part of the atmosphere indicating that the temperature remains essentially constant. In addition, the occultation measurements have provided information about ionospheric peak density and altitude. In the light of this new information, it was desirable to modify our previous model atmosphere of Mars and attempt a characterization of the Martian ionosphere. The neutral particle distribution was obtained by considering the photochemistry of carbon dioxide assuming that carbon dioxide is the predominant atmospheric constituent. For this purpose, the following reactions were considered:

$$CO_2 + h\nu \xrightarrow{\alpha_1} CO + O \qquad \lambda < 1750Å$$

$$CO + O \xrightarrow{k_2} CO_2$$

$$CO + O + M \xrightarrow{k_3} CO_2 + M$$

$$O + O + M \xrightarrow{k_4} O_2 + M$$

$$O_2 + h\nu \xrightarrow{\alpha_2} O + O \qquad \lambda < 2400Å$$

$$O + O_2 + M \xrightarrow{k_6} O_3 + M$$

$$O + O_3 \xrightarrow{k_7} 2O_2$$

$$O_3 + h\nu \xrightarrow{\alpha_3} O_2 + O \qquad \lambda < 3000Å$$

The other parameters employed in this study are given in Table 3. Three different cases are considered corresponding to three different temperatures and in each case, the atmosphere is assumed to be isothermal. It is also assumed that atmospheric mixing prevails up to the dissociation region and that diffusion sets in at a higher altitude where photodissociation is essentially complete. The previously-employed computer program was used also for the present study. The results for the neutral particle distributions thus obtained are shown in Figures 7, 8 and 9. It is evident that the temperature has an influence upon the peak altitude of dissociation.

These initial models were then employed to calculate the corresponding solar photoionization rate as a function of altitude for each individual constituent as well as the total rate. For this purpose, a numerical method of summation of various components was used. The photoionization rate, P, in ion-pairs/cm^3 sec at a given altitude was computed from the expression

$$P = \sum_{\lambda} I(\lambda, Z) \left[\sum \sigma_i(\lambda) n_i(Z) \right]$$

where $I(\lambda, Z)$ is the ionizing flux for a given wavelength interval at a given altitude, $\sigma_i(\lambda)$ is the average photoionization cross section for each constituent for a wavelength interval of 50Å, and $n_i(Z)$ is the number density for each constituent at the given altitude. To illustrate the data, the photoionization rates corresponding to Cases I, II and III are shown in Figures 10, 11 and 12, respectively. The ion density peaks are found to lie

TABLE 3

Parameter Employed for the Study of the Ionosphere of Mars

	Reference
Surface temperature	Kliore et al. (1965)
Case I - $T = 200^{o}K$	
Case II - $T = 180^{o}K$	
Case III - $T = 160^{o}K$	
Surface number density - 1.9×10^{17} molecule/cm^3	Kliore et al. (1965)
Solar flux on the top of the earth's atmosphere in 50Å intervals	
Wavelength Regions 3000 to 2550Å	Johnson (1954)
2500 to 1550Å	Detwiler et al. (1961)
1550 to 50Å	Hinteregger (1965)
Average dilution factor to account for the diminution of solar flux in the vicinity of Mars, $\mu = 0.444$	
Absorption Cross Sections	
Carbon Dioxide Oxygen Ozone	Sullivan and Holland (1966)
Photoionization Cross Sections	
Carbon Monoxide	Cairns and Samson (1965)
Atomic Oxygen	Dalgarno, Henry & Stewart (1964)
Carbon Dioxide	Romand (1962) Cairns and Samson (1965) Sun and Weissler (1955)
Photodissociation yield factors for oxygen, ozone, and carbon dioxide and photoionization yield factors for carbon monoxide, atomic oxygen and carbon dioxide are assumed to be unity	
$k_2 = 1.6 \times 10^{-14} \exp\left(-\frac{4000}{RT}\right)$ cm^3/sec	Mahan and Solo (1962)
$k_3 = 0$	
$k_4 = 2.8 \times 10^{-33}$ cm^6/sec	Morgan and Schiff (1963)
$k_6 = 5 \times 10^{-35} \exp\left(\frac{1000}{RT}\right)$ cm^6/sec	Benson and Axworthy (1957) as corrected by Jones and Davidson (1962)
$k_7 = 5 \times 10^{-11} \exp\left(-\frac{5600}{RT}\right)$ cm^3/sec	

REFERENCES TO TABLE 3

Kliore, A., D. L. Cain, G. S. Levy, V. R. Eshleman, G. Fjelbdo, and F. D. Drake — "Occultation Experiment: Results of the First Direct Measurement of Mar's Atmosphere and Ionosphere" Science, 1243-1248 (September 1965).

Johnson, F. S. — "The Solar Constant," J. Meteorol. 11, 431-439 (1954).

Detwiler, C. R., D. L. Garrett, J. D. Purcell, and R. Tousey — "The Intensity Distribution in the Ultraviolet Solar Spectrum," Ann. Geophys. 17, 263 (1961).

Hinteregger, H. E. — "Absolute Intensity Measurements in the EUV Spectrum of Solar Radiation," Space Science Reviews 4, 461-497 (1965).

Sullivan, J. O. and A. C. Holland — "A Congeries of Absolute Absorption Cross Sections for Wavelengths less than 3000Å," GCA Technical Report Number 64-20-N Contract Number NASw-840 (1964), NASA CR-371 (1966).

Cairns, R. B. and J. A. R. Samson — "Absorption and Photoionization Cross Sections of CO_2, CO, A, and He at Intense Solar Emission Lines," J. Geophys. Res. 70, 99 (1965).

Dalgarno, A., R. J. W. Henry, and A. L. Stewart — "Photoionization of Atomic Oxygen," GCA Technical Report Number 64-1-N, Contract Number NASw-840 (1964).

Romand, J. — Private communication (1962).

Sun, H. and G. L. Weissler — "Absorption Cross Sections of Carbon Dioxide and Carbon Monoxide in the Vacuum Ultraviolet," J. Chem. Phys. 23, 1625 (1955).

Mahan, B. H. and R. B. Solo — "Carbon Monoxide-Oxygen Atom Reactions," J. Chem. Phys. 37, 2669 (1962).

Morgan, J. E. and H. I. Schiff — "Recombination of Oxygen Atoms in the Presence of Inert Gases," J. Chem. Phys. 38, 1495 (1963).

Benson, S. W. and A. E. Axworthy — "Mechanisms of the Gas Phase Thermal Decomposition of Ozone," J. Chem. Phys. 26, 1718 (1957).

Jones, W. M. and N. Davidson — "The Thermal Decomposition of Ozone in a Shock Tube," J. Am. Chem. Soc. 84, 2868 (1962).

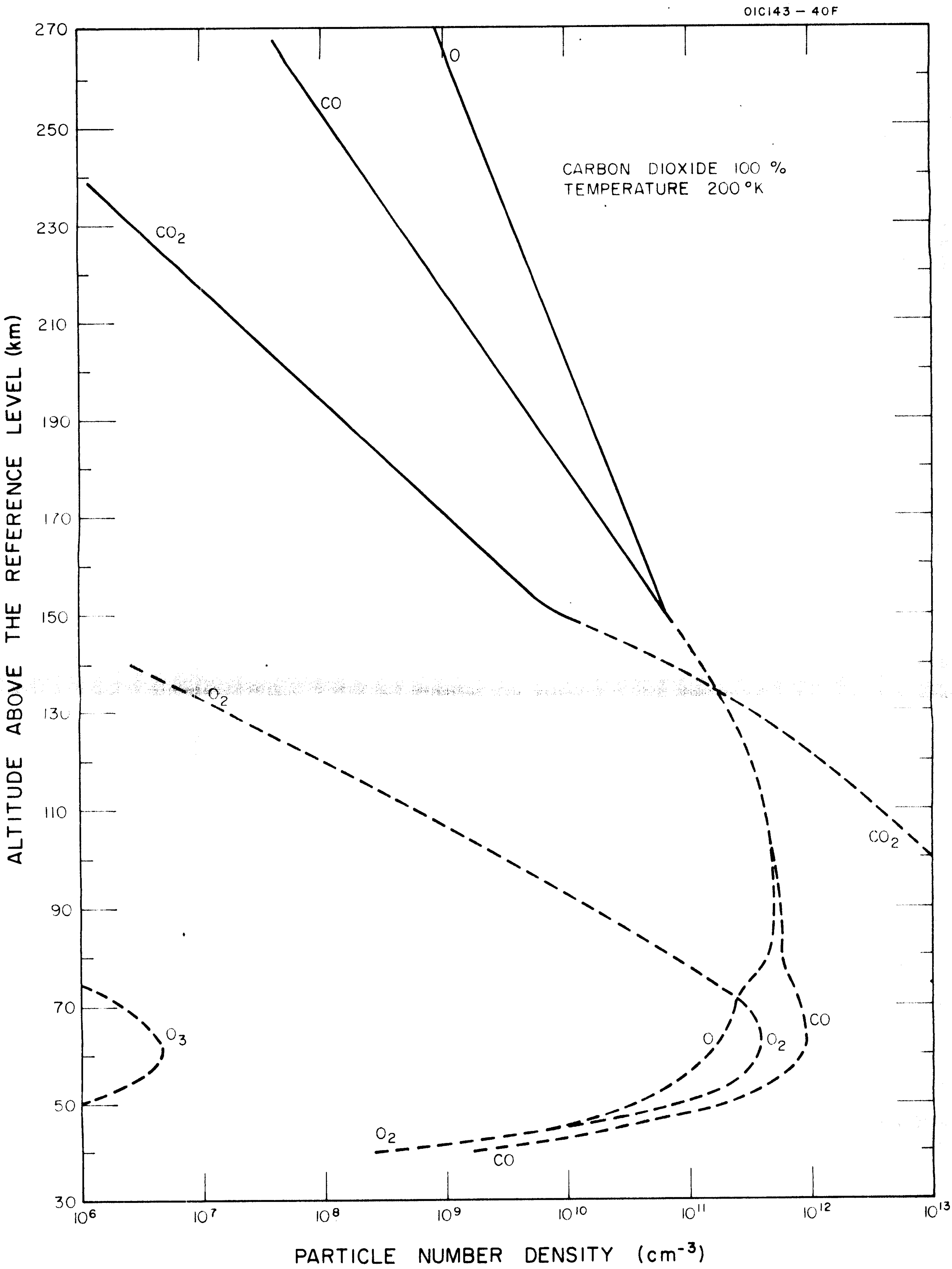

Figure 7. Neutral particle model atmosphere of Mars. Dotted lines are due to photochemical processes and the solid lines indicate the region of diffusion.

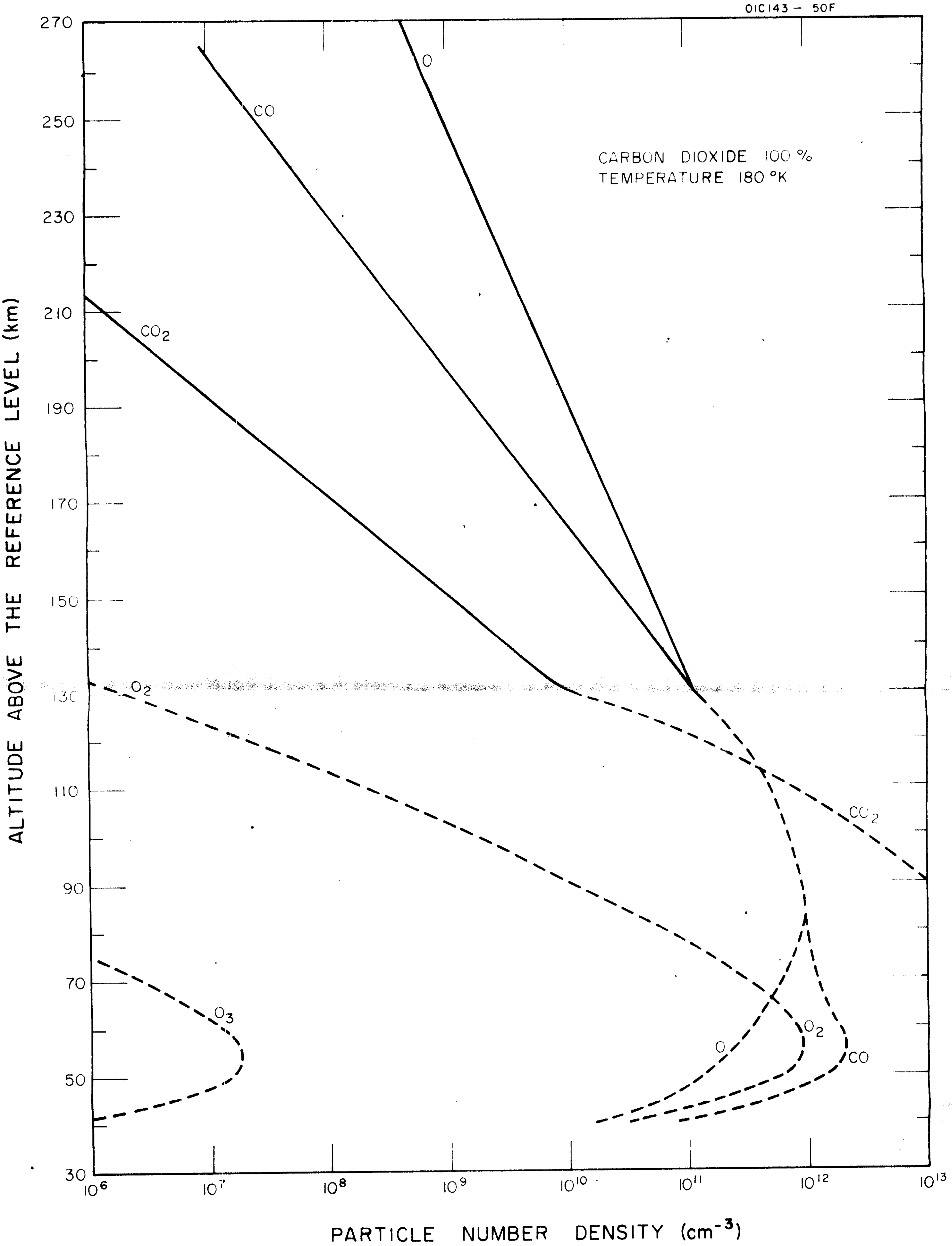

Figure 6. Neutral particle model atmosphere of Mars. Dotted lines are due to photochemical processes and the solid lines indicate the region of diffusion.

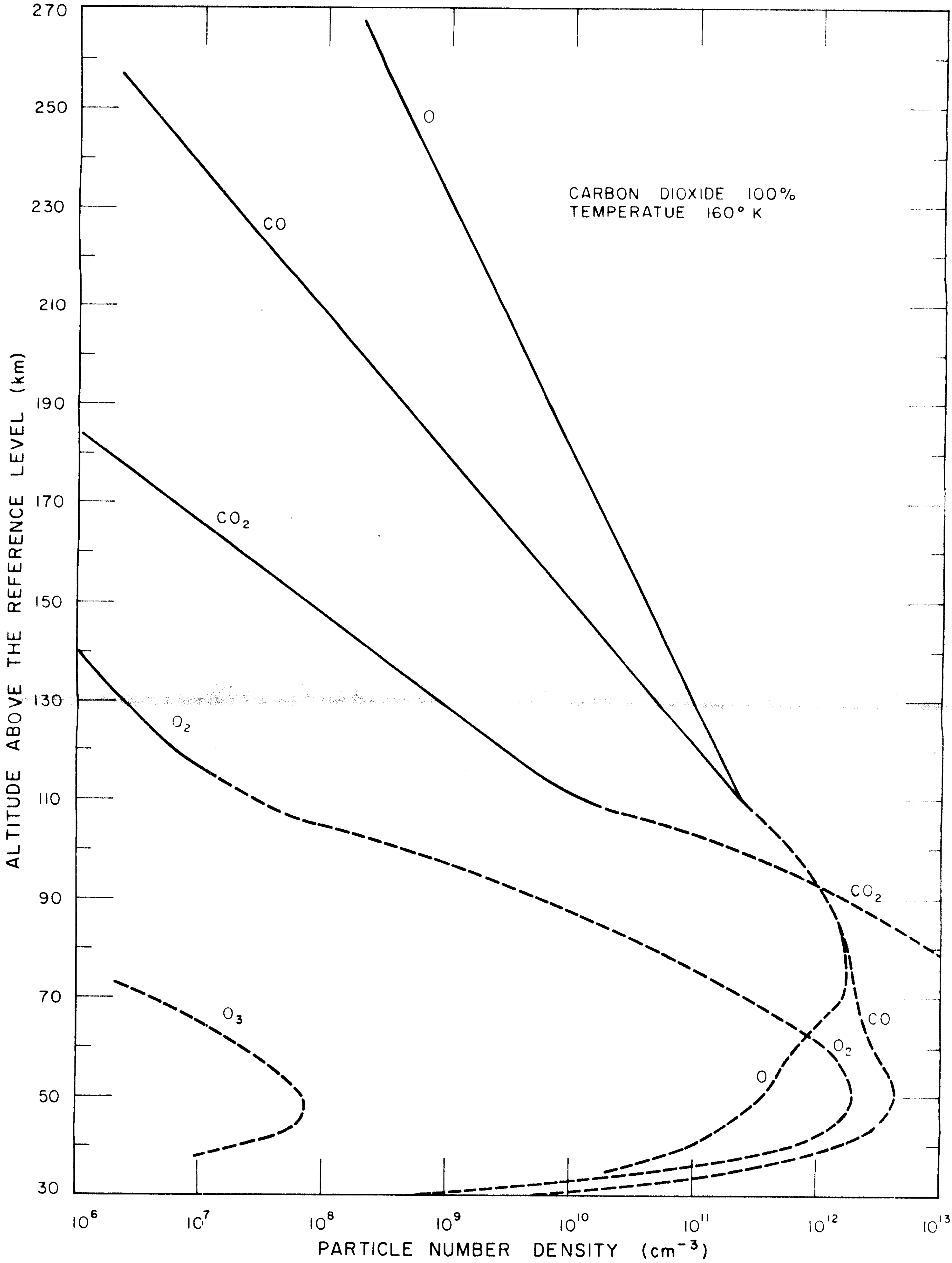

Figure 9. Neutral particle model atmosphere of Mars. Dotted lines are due to photochemical processes and the solid lines indicate the region of diffusion.

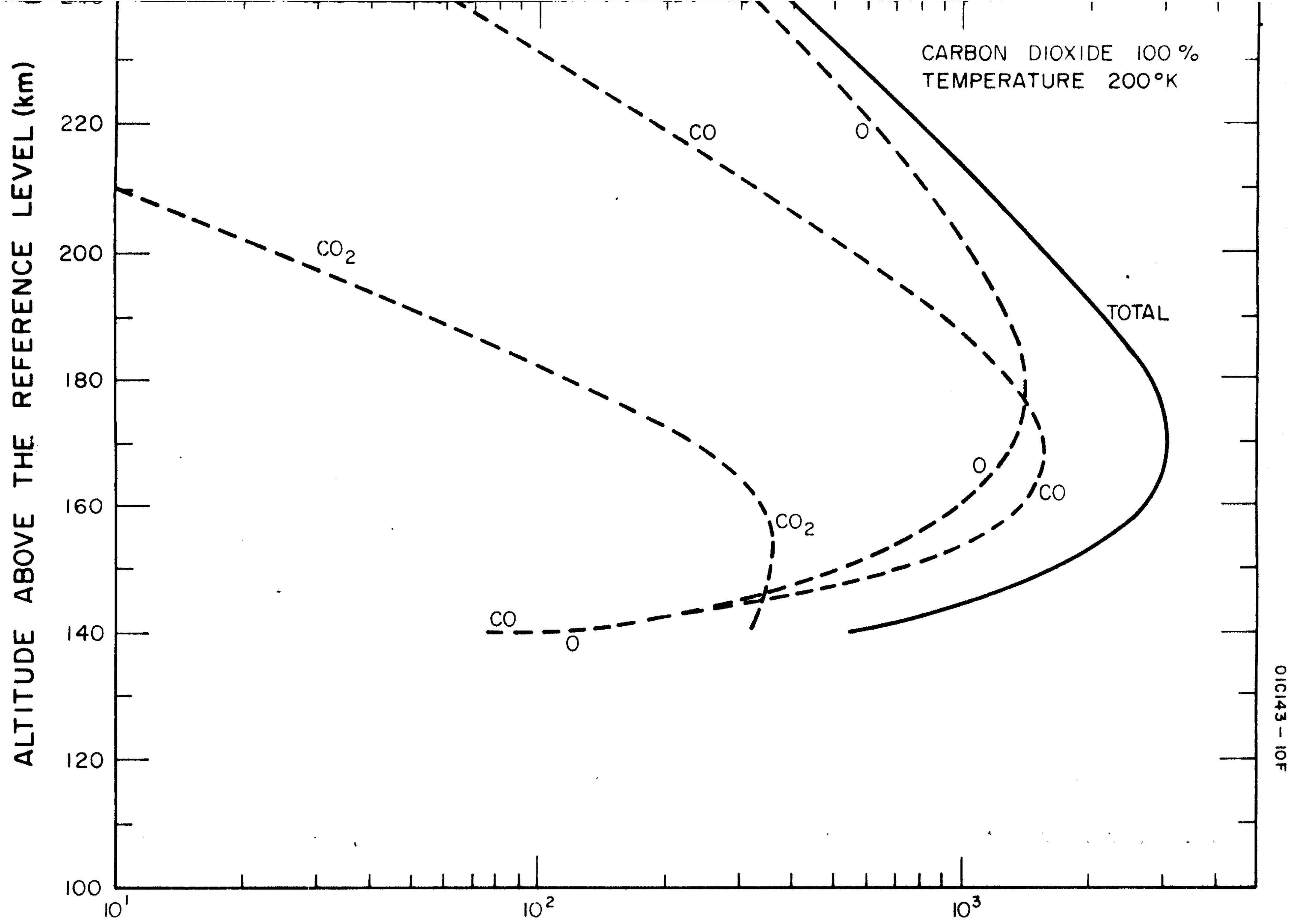

Figure 10. Photoionization rates for the atmosphere of Mars.

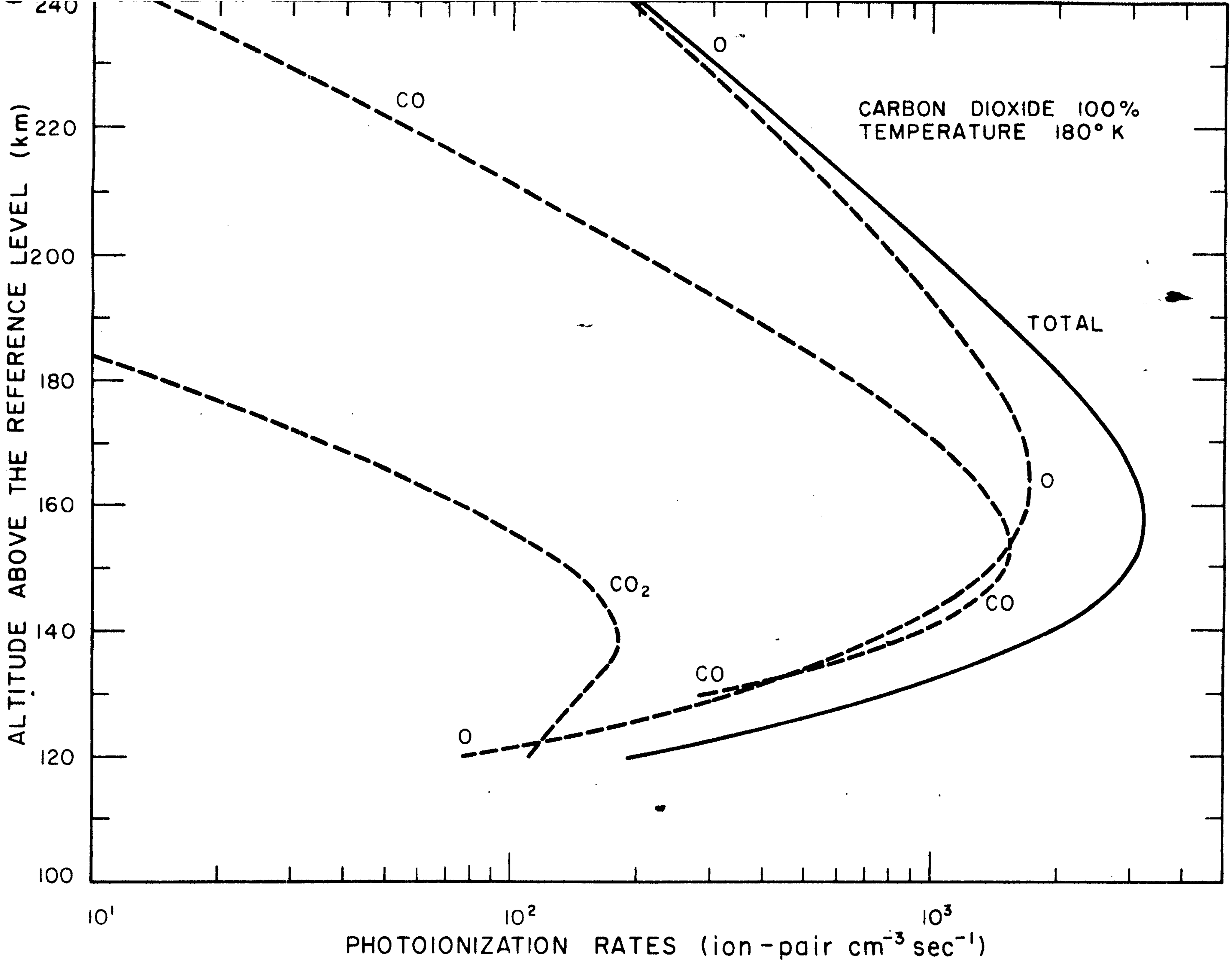

Figure 11. Photoionization rates for the atmosphere of Mars.

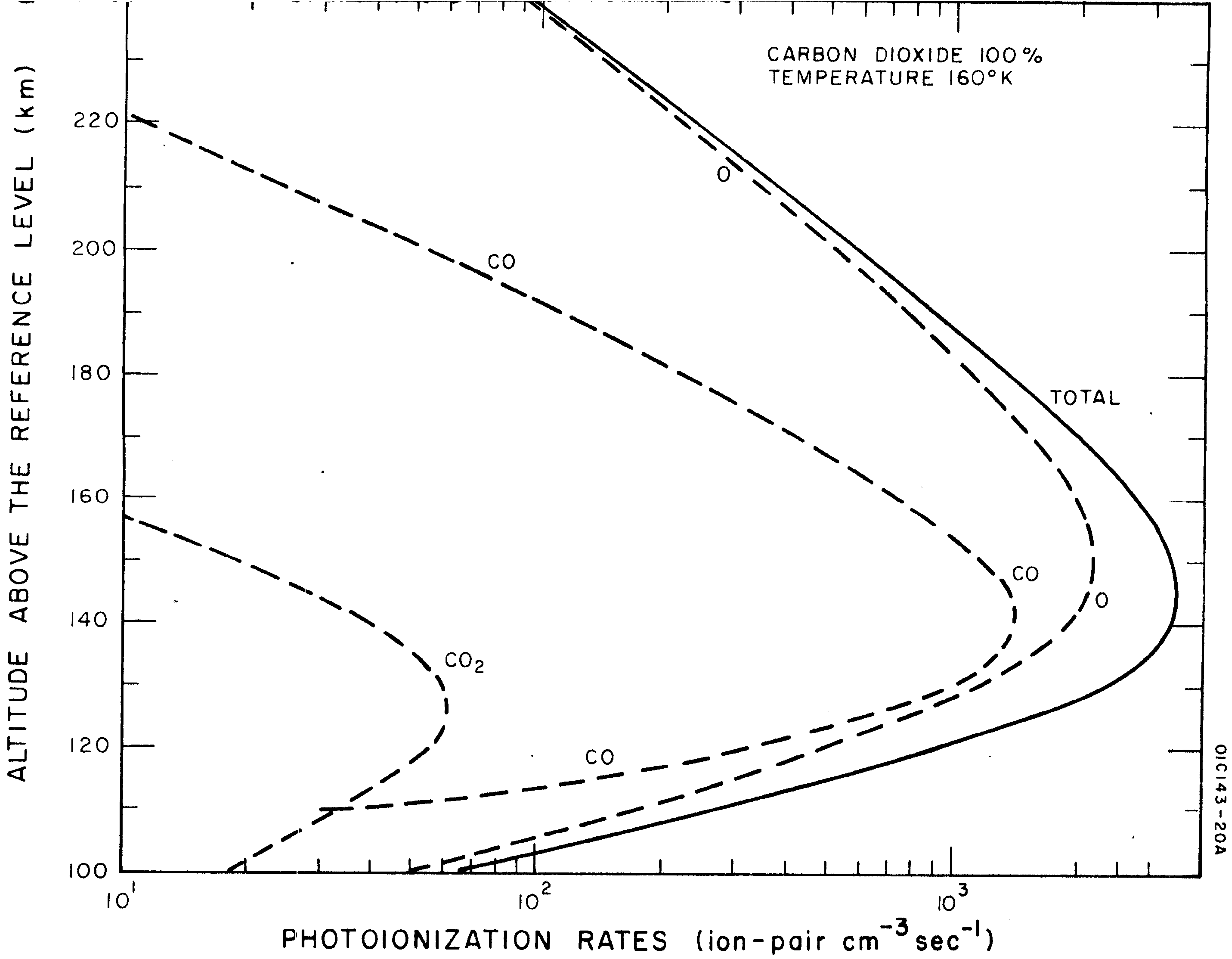

Figure 12. Photoionization rates for the atmosphere of Mars.

at 170, 160, and 145 km for the parameters employed and show that these peaks are higher than the ionization peak at 120 to 125 km observed in the Mariner IV experiment. This apparent discrepancy can be ascribed to several alternative shortcomings in the present model. A further clarification of the problem is currently being investigated.

b. A Satellite Experiment on the Detection of Noctilucent Clouds in the VUV Region

One of the requirements in the present program is to investigate the role of interplanetary debris deposited in the earth and planetary atmospheres. Previous efforts have been described in other Quarterly Rejorts in which the role of the vaporized atomic and/or ionized portions of the debris were considered. However, an important aspect of this problem includes the role of the remaining meteoric debris; i.e., that which survives during its flight through the earth atmosphere to become micrometeorite particles.

In this regard, Chapman and Kendall[13] have recently presented rather convincing arguments to show that the formation of noctilucent clouds can be directly related to the continuous influx of meteoric debris into the earth's atmosphere. Indeed, many other investigators also concur on the importance of the role of meteoric debris in the formation of noctilucent clouds. However, it is generally accepted that there is a lack of experimental observations. One reason for this is that earth-based operations are severely limited in that measurements can be obtained only under highly-restrictive conditions so that a requirement to detect noctilucent clouds (or dust layers) present in the earth's atmosphere on a global scale by a satellite-borne device becomes self-evident.

During the present Quarter, calculations were performed to determine the feasibility of performing such a satellite experiment by taking full advantage of the opportunity of probing in the vacuum ultraviolet region. Partial support of this phase of the program was also obtained under Contract No. NASw-1292 since there is close correlation with meteorological phenomena.

The study has indicated that the VUV region is an optimum region to explore and that there exists a high probability of noctilucent clouds in the wavelength region 1800 to 2000Å. A brief description of this work follows.

First, it is of prime importance to establish the ambient VUV background radiation from the solar-illuminated earth atmosphere. The nature and intensity of this background is not well known except for some isolated strong resonance lines. However, it is evident that several possible sources of radiation exist. Among these, the diffuse reflection of solar ultraviolet by Rayleigh scattering is probably the major contributor for the wavelength region of interest here (i.e., 1800 to 2000Å). Accordingly, in view of the complete lack of appropriate experimental data, a theoretical estimate of the background is obtained by calculating the expected VUV scattering background due to a solar-illuminated earth atmosphere throughout the spectral region of about 1100 to 2000Å.

The geometry of the problem is illustrated in Figure 13, where the solar flux is shown to be incident on top of a semi-infinite plane parallel atmosphere at an angle θ_o to the vertical. The radiation detector is assumed located above the atmosphere and looking downward in the direction

01DA130-40S

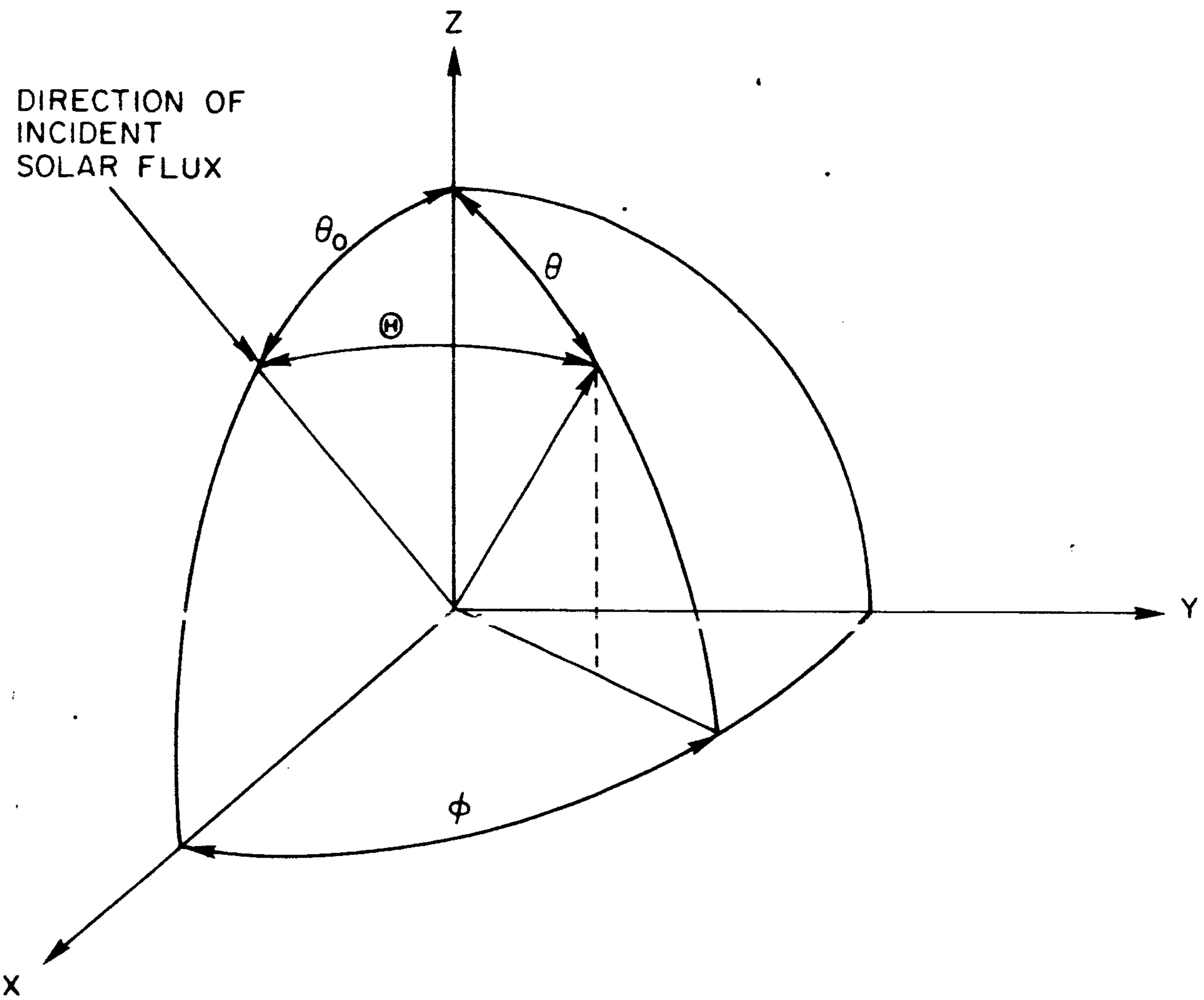

TOP OF ATMOSPHERE IN XY PLANE

SOLAR FLUX INCIDENT IN XZ PLANE AT ANGLE θ_o WITH RESPECT TO Z AXIS

REFLECTED RADIATION AT ANGLE θ WITH RESPECT TO Z AXIS, AZIMUTHAL ANGLE ϕ MEASURED IN XY PLANE FROM X AXIS

Figure 13. Geometry for diffuse reflection of solar radiation by a semi-infinite plane parallel atmosphere.

θ. The azimuth angle, ϕ, is defined as the angle between the direction of the incident solar flux and the diffusely-reflected ray. The angle between the incident solar flux and the ray reflected to the detector is Θ and is defined by

$$\cos \Theta = \cos \theta \cos \theta_o + \sin \theta \sin \theta_o \cos \phi \ . \tag{13}$$

The directions θ and θ_o have been selected so that the angles lie between 0 and $\frac{\pi}{2}$ radians. Since it can be shown that higher scattering orders can be neglected in the vacuum ultraviolet, the analysis has been limited to consideration of primary and secondary scattering.

The mathematical techniques required to compute the diffusely-reflected signal levels are complex, but essentially follow the scheme of Chandrasekhar.[14] Additionally, the model terrestrial atmosphere due to Champion[15] was adopted with minor modifications. Ozone concentrations inferred from the measurements of Dütsch[16] were added to the above model for computational purposes. Absorption cross sections for N_2, O_2, O_3 and CO_2 were obtained from the compilation of Sullivan and Holland,[17] whereas the Rayleigh scattering cross sections for N_2 were obtained from the experimental results of Marmo and Mikawa,[18] and from the results of Wilkinson.[19] For O_2, the Rayleigh scattering cross section at 1100Å was assumed to be 4.3×10^{-22} cm^2 which, when combined with the data of Landolt-Bornstein,[20] yielded appropriate values over the spectral region of interest.

The results of the above computations performed on an IBM 1620 computer are shown in Figure 14 for $\theta = \theta_o = 0^o$ (seen overhead

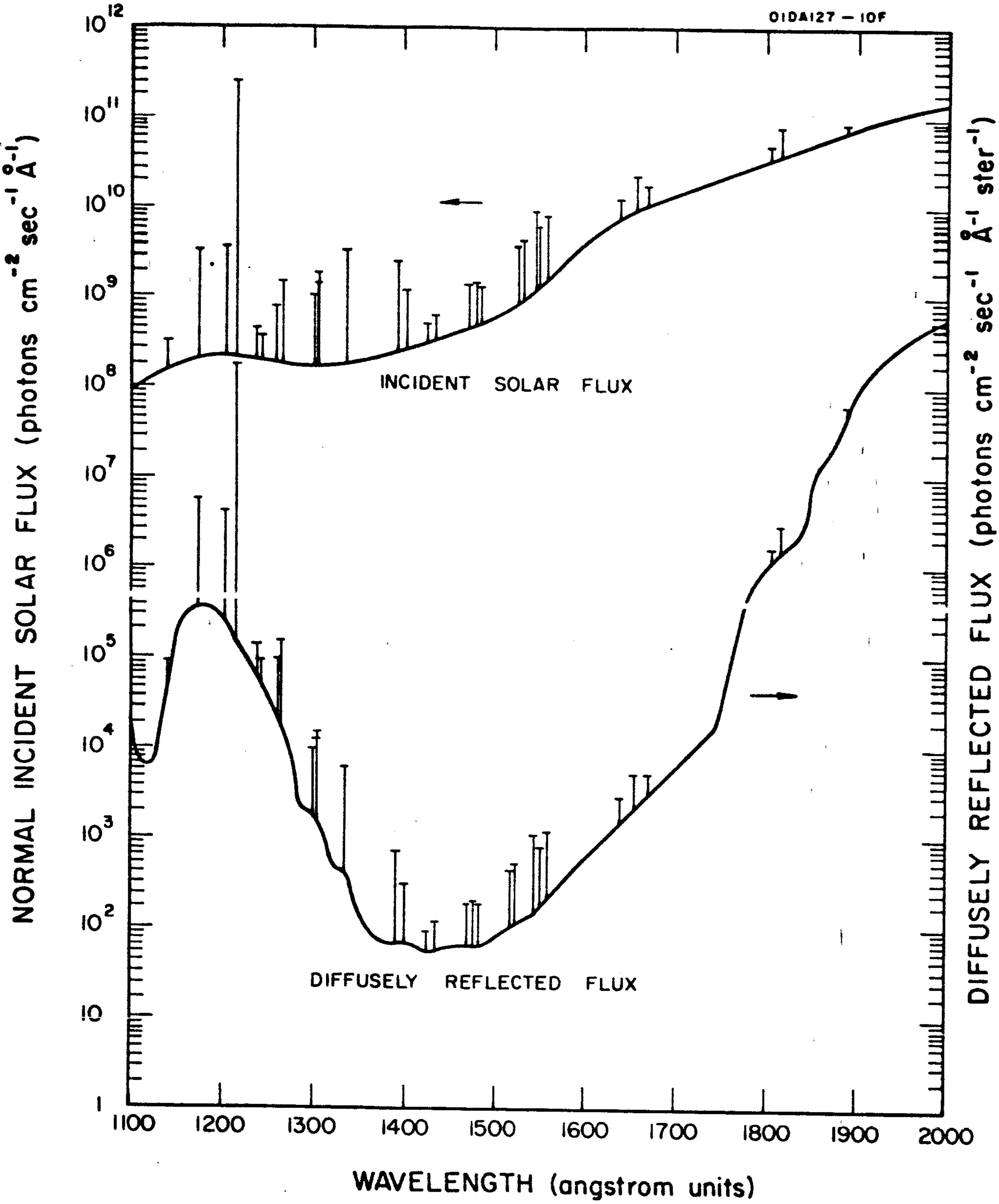

Figure 14. Comparison of incidence solar flux and vertically reflected flux in the vacuum ultraviolet.

and with the detector looking straight down). Results for other solar zenith angles and detector nadir angles can be obtained by the inclusion of the appropriate modifying trigonometric function. This is the background against which the signal must be observed.

Concerning the signal, it is of interest to point out that there is a strong variation of detectability altitude with wavelength in this spectral region. This is made evident by the data shown in Figure 15. One may take advantage of this situation for altitude discrimination in the observation of dust layers in the earth's atmosphere. The expected signal intensities from a typical noctilucent cloud have been estimated in order to evaluate the feasibility of this technique and to identify the pertinent experimental problems. For this purpose, we employed the data of Hemenway et al.[21] who have recently determined the size distribution of particles in a noctilucent cloud by an in situ rocket measurement (see Figure 16). It was shown that only about 10 percent of the particles have diameters $< 0.05\mu$ while fewer than 1 percent have diameters which exceed 0.3μ. Hemenway et al.[21] have concluded that particles whose diameters were $> 0.01\mu$ were probably ice-coated and that the ice coating diameter is about five times greater than that of the nucleus. Mie scattering calculations have been applied for the range of particle size indicated in Figure 16. The complex mathematical techniques and computations are not described here; however, they may be briefly described as a modification of the treatments due to Stratton[22] and van de Hulst[23] in which the dimensionless Mie scattering parameter, $x = 2\pi r/\lambda$, is employed throughout. In Figures 17 and 18 are plotted the computed angular Mie scattering coefficient as defined by

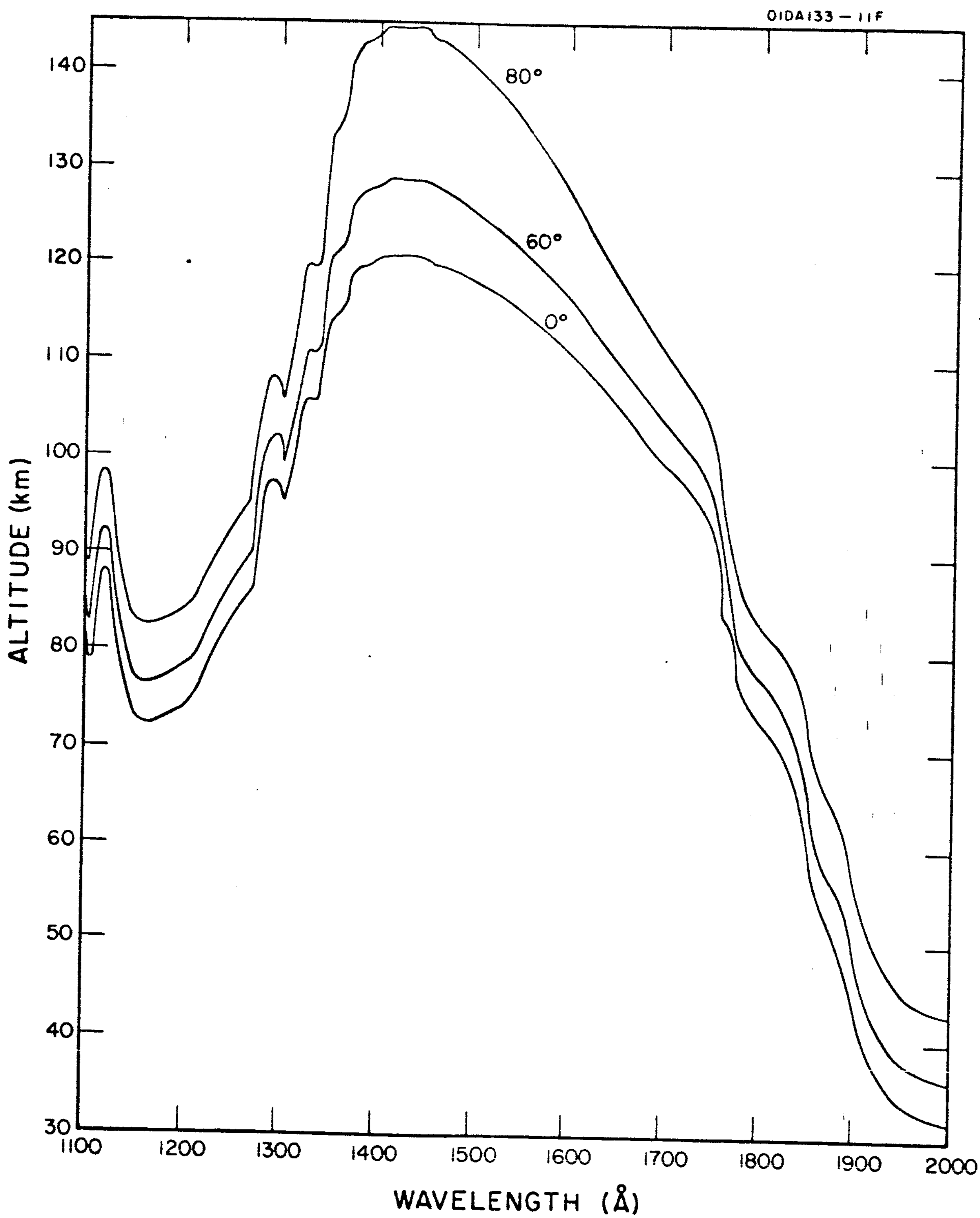

Figure 15. Altitude of unit optical thickness in the atmosphere in the vacuum ultraviolet for zenith angles 0,60, and 80 degrees.

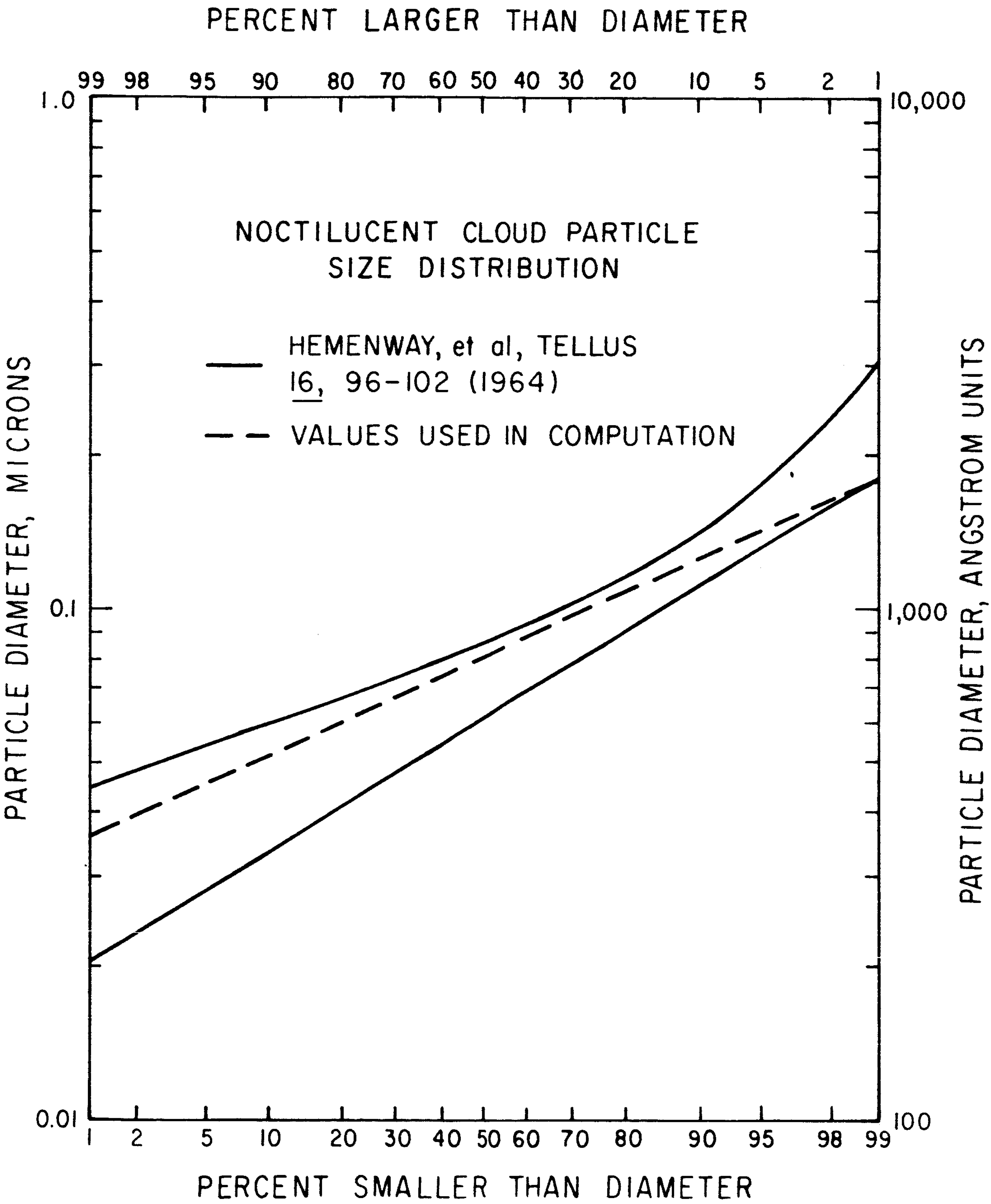

Figure 16. Size distribution of noctilucent cloud nuclei.

OIDA141-40F

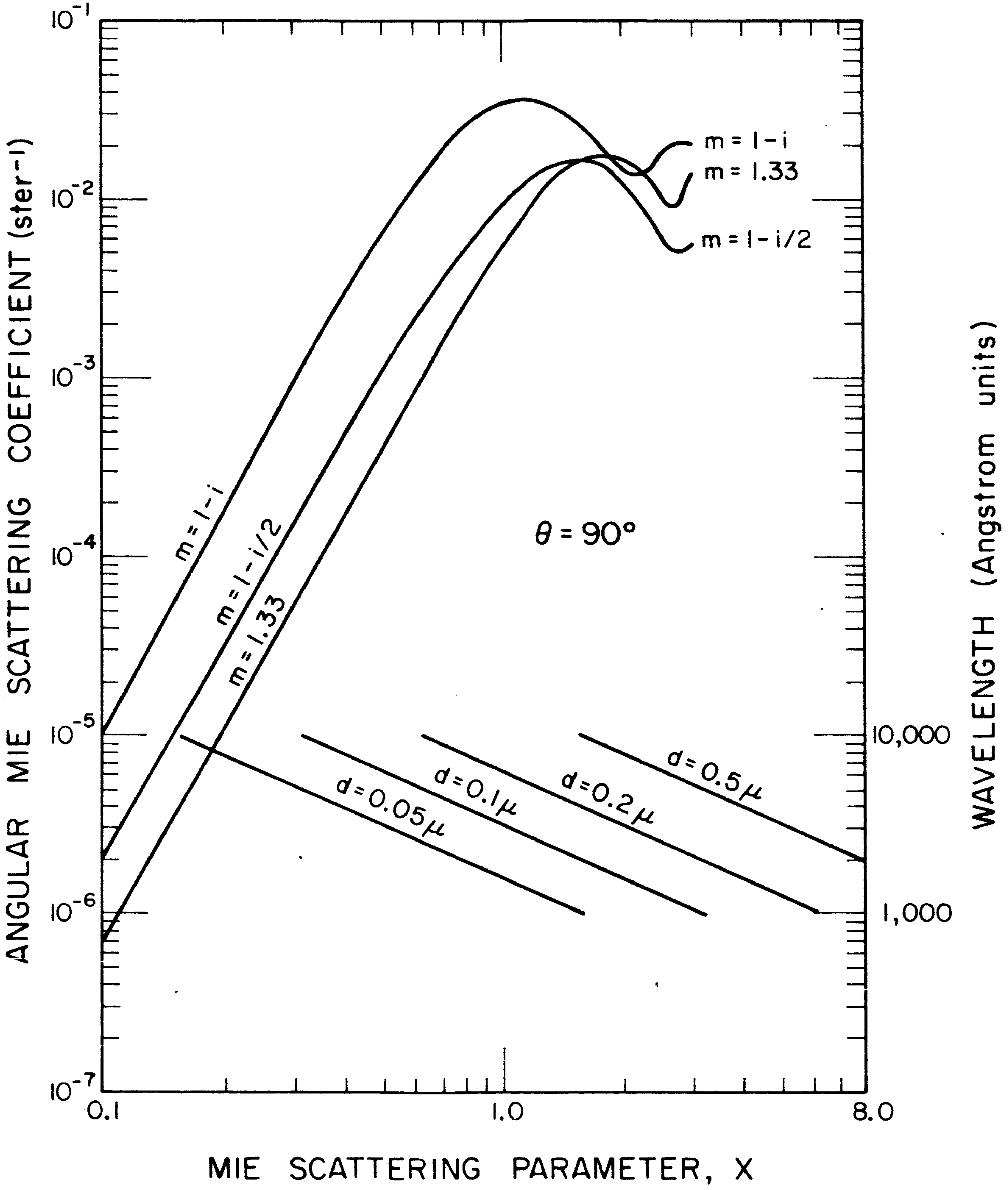

Figure 17. Mie angular scattering coefficient for spheres with refractive indices 1 - i, 1 - i/2 and 1.33. Scattering angle 90 degrees.

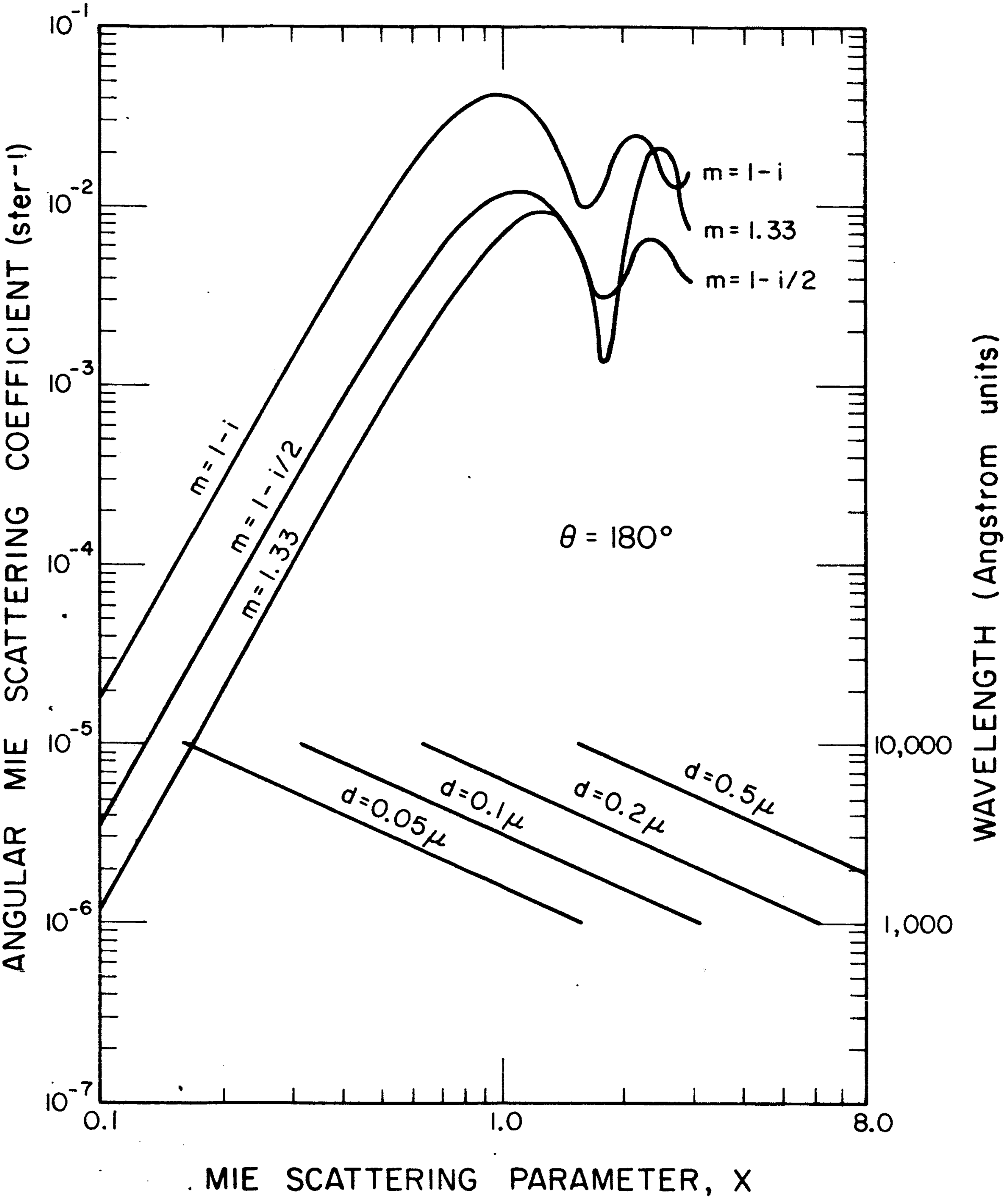

Figure 18. Mie angular scattering coefficient for spheres with refractive indices 1 - i, 1 - i/2 and 1.33. Scattering angle 180 degrees.

Penndorf[24] for scattering angles of 90 degrees and 180 degrees, respectively. Finally, Figure 19 shows the average angular scattered cross sections in cm^2/ster integrated over the assumed size distribution at a wavelength of 2000Å as a function of refractive index. It should be emphasized at this point that again there is a virtual lack of pertinent experimental measurements so that these computed values should be viewed with some caution.

The arguments which employ these data to illustrate the feasibility of the proposed satellite experiment are lengthy and not repeated here since the subject matter will be given in detail in a forthcoming GCA Technical Report. In any case, it has been demonstrated that for the reasonable estimates employed, a successful experiment can be performed by a satellite-borne Fastie-Ebert spectrometer for observing noctilucent clouds in the restricted spectral region $\lambda\lambda$ 1800 to 1900Å.

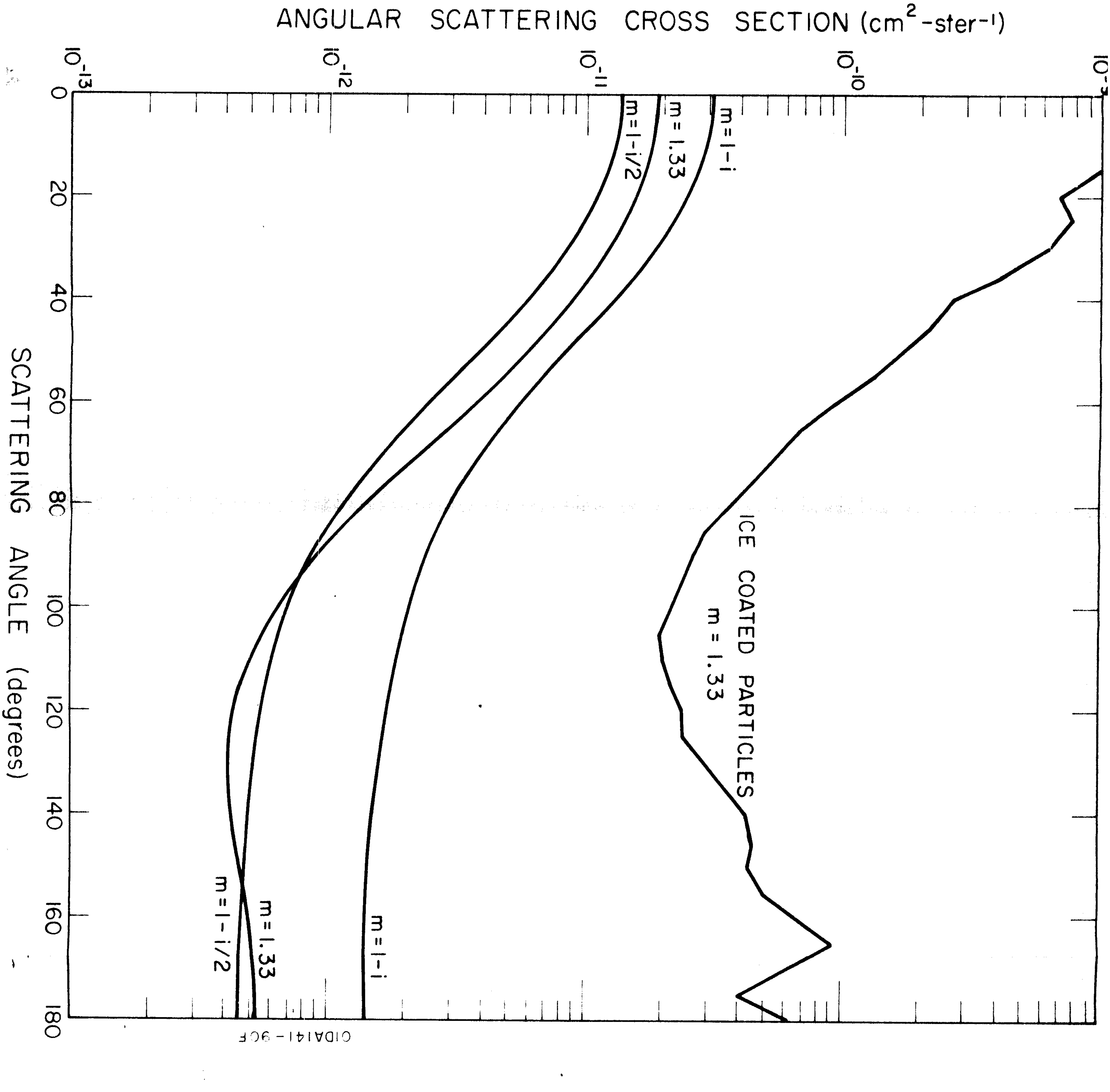
ANGULAR SCATTERING CROSS SECTION (cm^2-ster^{-1})
10^{-13}
10^{-12}
10^{-11}
10^{-10}
SCATTERING ANGLE (degrees)
0
20
40
60
80
100
120
140
160
180
m = 1-i/2
m = 1.33
m = 1-i
ICE COATED PARTICLES
m = 1.33

III. OTHER PERTINENT INFORMATION

During this Quarter, a technical paper entitled "A Study of the Kinetic Energies of Electrons Produced by Photoionization" by J.A.R. Samson and R. B. Cairns was presented by J.A.R. Samson at the Fiftieth Anniversary Meeting of the Optical Society of America on March 17, 1966, in Washington, D. C. The major invited papers of interest were presented by Professor Edlen on spectroscopy, Dr. Tousey on space and solar research, and Professor Garton on atomic physics and its applications to astrophysics. At the National Bureau of Standards, a team of theoretical physicists headed by Dr. U. Fano are vitally interested in the results produced by our Experimental Physics Department. They have written some theoretical papers on the photoionization cross sections of diatomic molecules based on the publications of our values of the absorption cross sections of H_2, N_2 and O_2. They have requested all future results we may obtain, especially on the kinetic energies of photoelectrons. Dr. Marton, at the National Bureau of Standards, is measuring the optical constants of metals in the vacuum ultraviolet. He is using the duoplasmatron as a light source (detailed drawings supplied by GCA), and credits GCA with their success since they had no suitable light source and no "know how." Dr. Behring of the Solar Physics Branch at NASA-Goddard Space Flight Center has been using the GCA absorption cross-section values for N_2, O_2 and O for analysis of their satellite data on number densities.

Labor Category	Labor Grade	Total Hours
*Junior Technician	2	303.00
*Technician Experimental Machinist	3	138.00
*Senior Technician Senior Experimental Machinist	4	491.50
*Junior Scientist Junior Engineer	5	296.50
*Scientist Engineer	6	374.50
Senior Scientist Senior Engineer	7	741.00
Staff Scientist	8	459.00
Principal Scientist	9	179.00
Group Scientist	10	108.00
ODC (Overhead Direct Charges)	6	75.00
" " " "	10	120.00

*and other equivalent categories.

REFERENCES

1. Hunten, D.M. and M.B. McElroy, Contribution No. XXX from Kitt Peak National Observatory, Tucson, Arizona (1965).

2. Kvifte, G. and L. Vegard, Geofys. Publ. 17. No. 3 (1947).

3. deMore, W. and O.F. Raper, J. Chem. Phys, 37, 2048 (1962).

4. Warneck, P., Disc. Faraday Soc. 37, 57 (1964).

5. Warneck, P., J. Chem. Phys. 41, 3435 (1964).

6. deMore, W. and O.F. Raper (to be published).

7. Norrish, R.G.W. and R.P. Wayne, Proc. Roy. Soc. A288, 200 (1965).

8. Cvetanovic, R.J., J. Chem. Phys. 43, 1850 (1965).

9. Kistiakowsky, G.B. and L.W. Richards, J. Chem. Phys., 36, 1707 (1962).

10. Hand, C.W., J. Chem. Phys., 36, 2521 (1962).

11. Jonathan, N., F.F. Marmo and J.P. Padur, J. Chem. Phys. 42, 1463 (1965).

12. Tanaka, Y., A.S. Jursa and F.J. LeBlanc, The Threshold of Space, M. Zelikoff, Ed., Pergamon Press, Ltd., London, England, pp. 89-93 (1957).

13. Chapman, S., and P.C. Kendall, "Noctilucent Clouds and Thermospheric Dust: Their Diffusion and Height Distribution," Quarterly Journal Roy. Meteorological Soc. 91, 115-131 (1965).

14. Chandrasekhar, S., Radiative Transfer, Dover Publication, New York (1960).

15. Champion, K.S.W., "Mean Atmospheric Properties in the Range 30 to 300 km," Air Force Surveys in Geophysics No. 164, AFCRL-65-443 (June, 1965).

16. Dütsch, H.V., "Vertical Ozone Distribution over Arosa," Tech. Rpt. No. 1 under Grants AF-BOARDC 61-18 and AF-EOAR 62-115, AFCRL 63-659 (1963).

17. Sullivan, J.O., and A.C. Holland, "A Congeries of Absorption Cross Sections for Wavelengths Less Than 3000Å," NASA CR-371 (January 1966).

REFERENCES (continued)

18. Marmo, F.F., and Y. Mikawa, "Scattering of Lyman-Alpha (1215.7Å) by Helium, Argon, Neon, Nitrogen and Hydrogen," Bull. Am. Phys. Soc. 9, 626 (1964).

19. Wilkinson, P.G., "Refractive Dispersion of Nitrogen in the Vacuum Ultraviolet," J. Opt. Soc. Am. 50, 1002 (1960).

20. Landolt-Bornstein, Zahlenwerte and Funktionen aus Physik, Chemie, Astronomie, Geophysik, aus Technik, Sixth Edition, Vol. 2. Part 8, pp. 871-893, Springer-Verlag, Berlin, Göttingen, Heidelberg (1962).

21. Hemenway, C.L., E.F. Fullam, R.A. Skrivanek, R.K. Soberman, and G. Witt, "Electron Microscope Studies of Noctilucent Cloud Particles," Tellus 16, 96-102 (1964).

22. Stratton, J.A., Electromagnetic Theory, McGraw-Hill, New York (1961).

23. van de Hulst, H.C., Scattering of Light By Small Particles, John Wiley and Sons, (1957).

24. Penndorf, Rudolph, "Angular Mie Scattering," J. Opt. Soc. Am. 52, 402-408 (1962).